APPRAISAL OF THE WATER RESOURCES OF THE EASTERN PART OF THE TULARE AQUIFER, BEADLE, HAND, AND SPINK COUNTIES, SOUTH DAKOTA

By Logan K. Kuiper

U.S. GEOLOGICAL SURVEY

Water-Resources Investigations Report 84-4078

Prepared in cooperation with the
SOUTH DAKOTA DEPARTMENT OF
WATER AND NATURAL RESOURCES

U.S. DEPARTMENT OF THE INTERIOR
March 3, 1849

Huron, South Dakota

1984

UNITED STATES DEPARTMENT OF THE INTERIOR

WILLIAM P. CLARK, Secretary

GEOLOGICAL SURVEY

Dallas L. Peck, Director

For additional information
write to:

District Chief, WRD
U.S. Geological Survey
Rm. 317, Federal Bldg.
200 4th St. SW
Huron, South Dakota 57350

Copies of this report can
be purchased from:

Open-File Services Section
Western Distribution Branch
U.S. Geological Survey
Box 25425, Federal Center
Denver, Colorado 80225
(Telephone: (303) 236-7476)

CONTENTS

ILLUSTRATIONS

ILLUSTRATIONS--Continued

APPENDIXES

CONVERSION FACTORS

For readers who may prefer to use metric units rather than inch-pound units, the conversion factors for the terms in this report are listed below:

Multiply	By	To obtain
acre	0.4047	hectare
acre-foot (acre-ft)	0.001233	cubic hectometer
foot (ft)	0.3048	meter
foot per day (ft/d)	0.3048	meter per day
foot per mile (ft/mi)	0.1894	meter per kilometer
cubic foot per day (ft^3/d)	0.02832	cubic meter per day
cubic foot per second (ft^3/s)	0.02832	cubic meter per second
gallon per minute (gal/min)	0.06309	liter per second
inch (in)	25.4	millimeter
inch per year (in/yr)	25.4	millimeter per year
mile (mi)	1.609	kilometer
square mile (mi^2)	2.590	square kilometer

National Geodetic Vertical Datum of 1929 (NGVD of 1929): A geodetic datum derived from a general adjustment of the first-order level nets of both the United States and Canada, formerly called mean sea level. NGVD of 1929 is referred to as sea level in this report.

APPRAISAL OF THE WATER RESOURCES OF THE EASTERN PART OF THE TULARE AQUIFER, BEADLE, HAND, AND SPINK COUNTIES, SOUTH DAKOTA

By Logan K. Kuiper

ABSTRACT

A system of glacial outwash aquifers lie in the central James Valley in east-central South Dakota. Within this system, the eastern part of the Tulare aquifer, which has an area of approximately 681 square miles, was simulated by means of a numerical ground-water flow model.

The model estimates the yearly average recharge rate for that part of the aquifer lying west of the James River to be approximately 23,000 acre-feet per year. The estimated 1978 yearly average irrigation pumpage rate was 9,800 acre-feet per year. It is expected that, since pumping will reduce discharge from the aquifer through evapotranspiration and flow to the James River, this part of the aquifer would be able to supply irrigation water at recent pumpage rates for an indefinite period. For that part of the aquifer lying east of the river, estimated recharge is 6,800 acre-feet per year. The estimated 1978 yearly average irrigation pumpage rate was 7,200 acre-feet per year. It is estimated that this part of the aquifer would be able to supply irrigation water at 7,200 acre-feet per year for approximately 50 years, at which time excessive drawdown would begin to cause reduced well yields at several locations.

INTRODUCTION

A system of glacial outwash aquifers used for irrigation lie in the central James valley in east-central South Dakota (fig. 1). The partially water-table glacial outwash aquifer of this study, the eastern part of the Tulare aquifer, is approximately outlined in figure 2 by aquifer model areas A and B.

Agriculture is the major economic base of the study area as it is for most of eastern South Dakota. The soil is for the most part very fertile. The principal restraining factor upon crop production is rainfall which averages only about 18.8 in/yr. The irrigation which is practiced in the area commonly doubles the yield of many crops.

The purpose of this study is to attempt to predict the ability of the aquifer to supply water for irrigation in the future. The main tool used for this purpose is a numerical ground-water flow model. Certain other methods will be mentioned which give less ambitious but useful predictions.

WATER USE

Irrigation use in the study area is presently at least 10 times larger than all municipal and domestic use. Thus the effects of all pumping except that of irrigation have been ignored in the aquifer model of this study. Irrigation use has increased

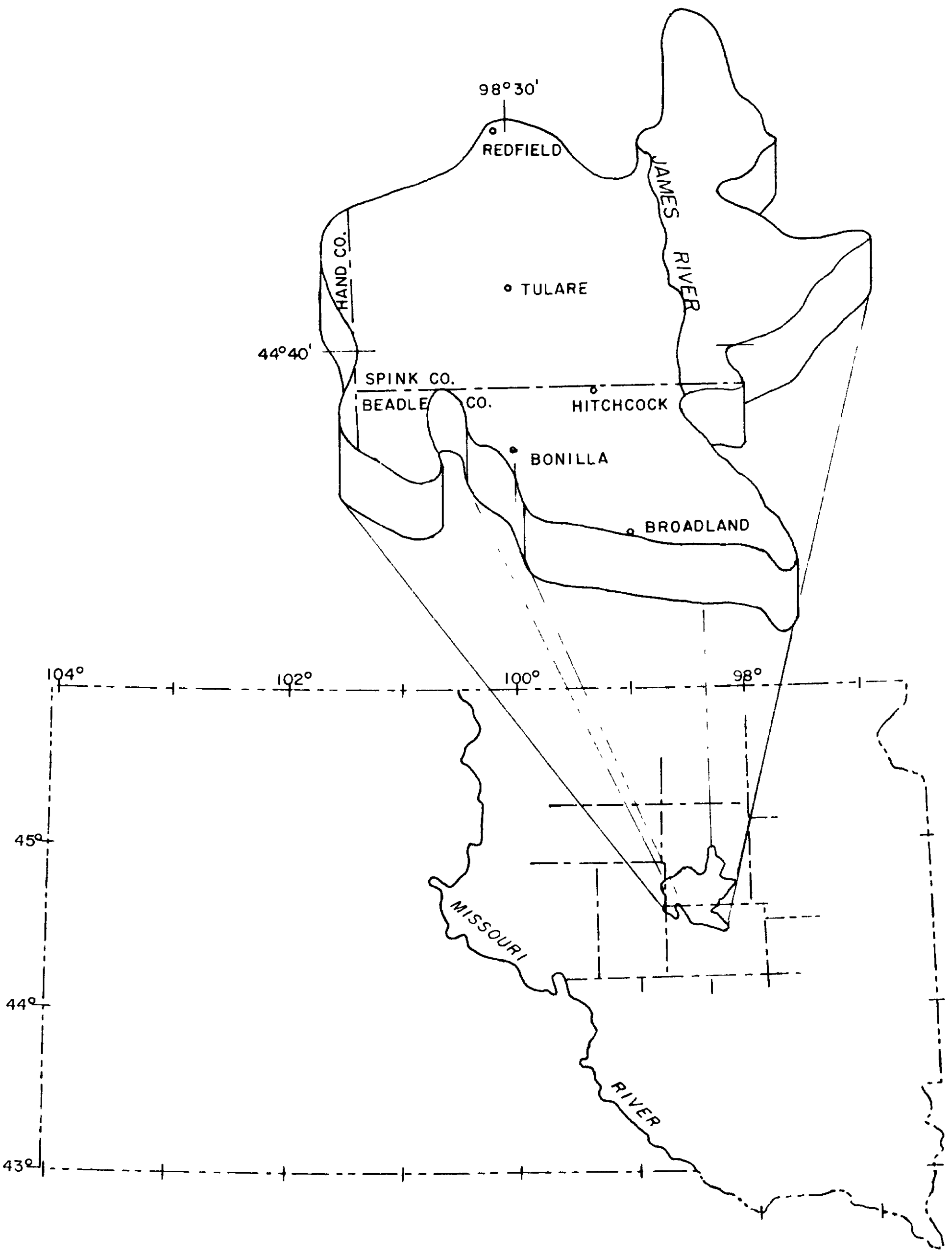

Figure 1.--Location of study area in east-central South Dakota.

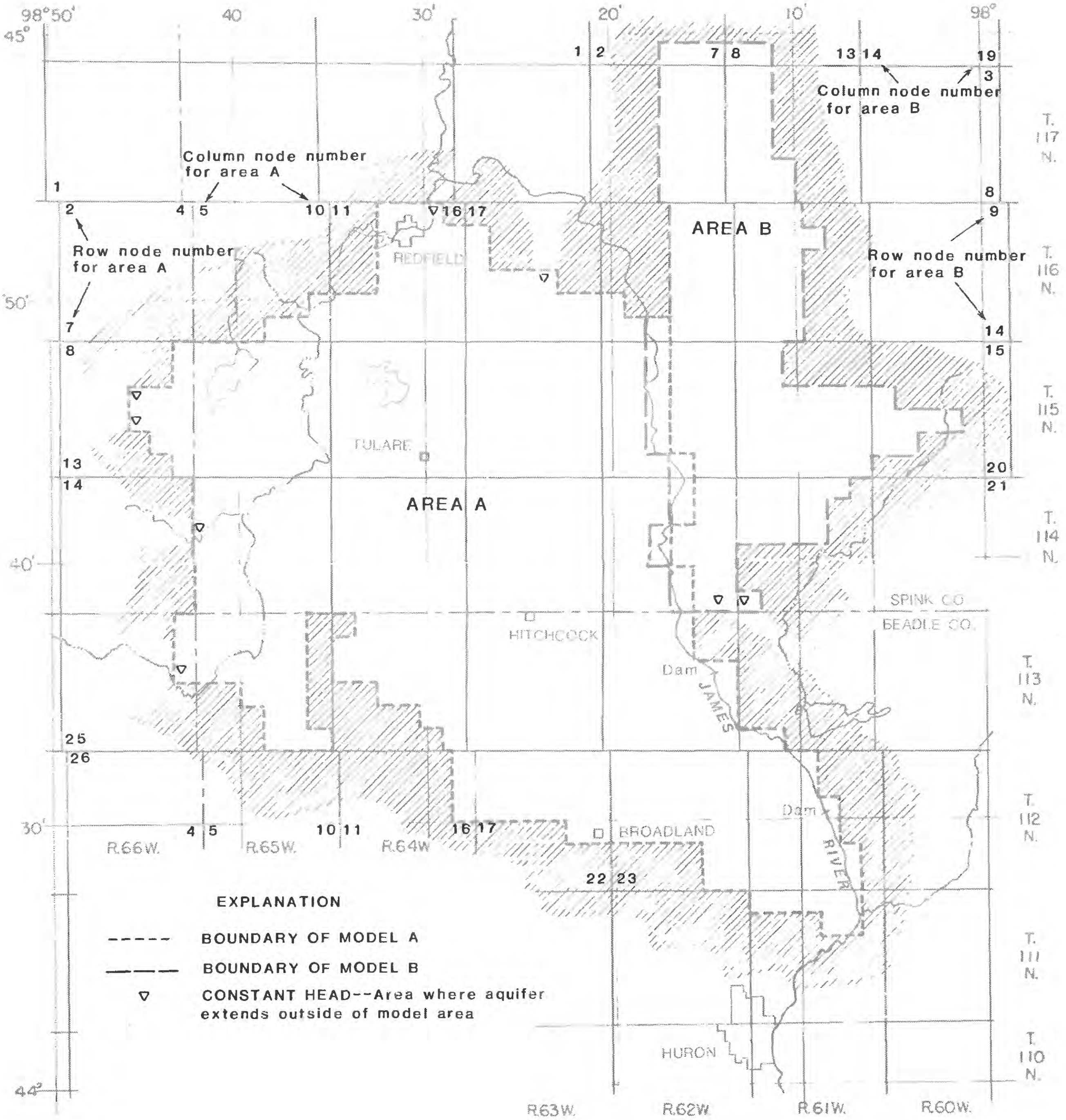

Figure 2.--Location of aquifer model areas.

remarkably in the last 10 years. In 1978, irrigation water-use questionnaires show that 8,173 acre-ft of water was applied in aquifer model area A as shown in figure 2, and 6,029 acre-ft was applied in aquifer model area B. Typical application rates are 8 to 20 inches per irrigation season. The application rate peaks in late summer with more than 50 percent of the total yearly amount occurring in the months of July and August. Almost all application is made by some type of sprinkler system. The center pivot irrigation system, covering a circular-shaped area with a radius of up to one-quarter mile, is the most common means of application.

HYDROGEOLOGY

Most surficial deposits in the study area are the result of glaciation of Pleistocene age and collectively are called drift. This drift can be divided into two major types, till and outwash, that differ greatly in physical and hydrologic characteristics. Till, which was deposited directly from or by glacial ice, is a heterogeneous mixture of silt, sand, gravel, and boulders in a matrix of clay. It is the most abundant glacial deposit in the area. Outwash, which was deposited from or by meltwater streams beyond the margin of active glacial ice, consists primarily of layers of clayey or silty sand and sandy gravel interbedded with layers of sandy and gravelly silt or clay. Beds of well-sorted sand and gravel are contained in the outwash.

The permeability of the till generally ranges from less than 0.001 to about 0.1 ft/d and the permeability of the outwash deposits generally ranges from less than 1 to more than 500 ft/d (Howells and Stephens, 1968).

The aquifer under consideration in this report consists of most of the eastern part of the Tulare aquifer, which itself is a small part of a complex system of outwash aquifers called the Central James aquifer complex by Howells and Stephens (1968). It has been chosen or segmented from the larger complex in such a way as to be fairly isolated hydrologically. Figure 2 shows several small areas near the fixed-head nodes where it is hydrologically connected with other parts of the Tulare aquifer.

The contact between the glacial deposits and older bedrock formations is characterized by the local presence of deeply incised drainage channels buried by overlying drift. In some locations the depth to bedrock may change by more than 300 ft within a horizontal distance of less than one-fourth mile. The location of these channels is not well known because few drill holes are deep enough to reach bedrock. The areal density of all drill holes in the 681-mi^2 area of the aquifer is approximately 2.3 holes per square mile. A channel draining the southern part of Spink County and presumably connecting with a deep channel headed northward in the extreme northern part of the county can not be located with the present drill hole data.

The surficial deposits in the study area are underlain by bedrock made up mostly of the Pierre Shale of Cretaceous age, which acts as a confining bed that permits the flow of only small amounts of ground water. The Pierre Shale is underlain by the Niobrara Formation and the Codell Sandstone Member of the Carlile Shale both of Cretaceous age. The Niobrara Formation and Codell Sandstone Member are aquifers, and are in contact with the Tulare aquifer in some of the deeper channels. The hydraulic head in these aquifers is usually not appreciably different from the hydraulic head in the surficial aquifers. Because of this fact, the fairly low permeability of these bedrock aquifers, and their apparent limited contact with the Tulare aquifer, the flow between the glacial and bedrock aquifers is ignored in this study.

A reliable delineation of the aquifer of this study is difficult to obtain because of the glacial processes that deposited the outwash making up the aquifer. Because the channels in the bedrock surface sometimes contain outwash, they further complicate the aquifer geometry. Certain areas were test drilled with a large density of wells, perhaps as many as 20 drill holes in a one-fourth square mile area, usually as part of a test program to find a suitable location for an irrigation well. The analysis of such high-density data shows that transmissivity can in some places change by orders of magnitude within a horizontal distance of less than one-half mile. Furthermore, within an area of less than one-fourth square mile, the aquifer can be a water-table aquifer at several locations and confined at several others. In one part of the area the aquifer may be separated by several till layers, at another part of the area have no till breaks, but at still another site within the area be totally absent.

The application of the aquifer model was made difficult by the heterogenity of the aquifer. The aquifer model requires the altitude of the top and bottom of the aquifer in each of the model nodes, which were chosen to be the 681 1-mi^2 sections in figure 2. For each of these 1-mi^2 nodes, the altitude of the top of the aquifer was chosen to be the average of the aquifer top altitudes from the drill hole data. The same procedure was used for the bottom altitude. Frequently, several different vertically spaced aquifer units, interspaced with low-permeability materials, are present. In this case, the top surface of the uppermost aquifer unit was used for the node's aquifer top altitude and the bottom surface of the lowermost aquifer for the node's aquifer bottom altitude. This procedure would seem to exaggerate the transmissivity of the aquifer in the model, because the thickness of the single aquifer in the model is greater than the total thickness of the aquifer units actually present. This thickness increase can be compensated, however, by reducing the value of the hydraulic conductivity for the node. However, the procedure may cause the aquifer model to give inaccurate results locally because, as the water level declines, it would give the same specific yield and hydraulic conductivity to the interspaced low-permeability materials as to the aquifer materials.

The average altitude of the bedrock beneath the aquifer is approximately 1,190 ft. From existing drill-hole data, the highest bedrock altitude is 1,309 ft and the lowest 845 ft. The average altitude of ground surface is approximately 1,290 ft, giving an average thickness of approximately 100 ft for the surficial deposits. The highest ground surface altitude is 1,304 ft and the lowest 1,235 ft. The average total thickness of the aquifer units is approximately 35 ft and the maximum total thickness from drill-hole data is 173 ft.

The ground surface is very flat. West of the James River, the ground surface slopes approximately northeast toward the James River with an average slope of approximately 7.3 ft/mi. Many of the 1-mi^2 sections show less than 10 ft of relief. Those that contain small streams or one of the numerous small ponds or marshy areas commonly show more relief. The James River flood plain is typically from 0.1 to 0.3 mi wide, and is flanked by hills that are approximately 25 to 40 ft high.

The water carried in streams in the study area is primarily surface runoff. Stream base flow originating in the study area is very small. Even the James River has a base flow from the aquifer below or in proximity with it which is too small to be measured. The result of this is that without irrigation, the hydrology of the aquifer is simply one of recharge in certain locations, movement of the water downgradient horizontally through the aquifer, and then upward movement through the overburden, whereupon evapotranspiration and a small amount of flow to streams occurs. The movement of water is from high ground-surface altitude areas, which are probably small depressions, to areas of low ground-surface altitude. These areas of low ground-surface altitude are typically areas adjacent to streams, ponds, or marshy areas. The James River flood plain alone probably receives approximately 20 to 30 percent of the total amount of water evapotranspirated and nearly all of the water discharged to streams. When irrigation effects are considered, some of the recharge water is routed to pumping wells instead of going to low areas for natural discharge. However, the James River flood plain still continues to receive water. It is assumed that drawdown is not sufficient to cause the river to become a source for irrigation water as is sometimes the case with other stream-aquifer systems.

THE AQUIFER MODEL

A generalized conceptualization of the total hydraulic system is depicted in figure 3. Note that the aquifer is only a part of this total system. The model of the aquifer, the main subject of this report, thus simulates only a part of the total hydrologic system. The mathematical procedure in the model used to simulate the aquifer is described by Trescott, Pinder, and Larson (1976), and is based upon the Darcy flow law for the movement of water in porous media and the conservation of the water passing into and out of each of the 1-mi^2 nodes of the aquifer model. The Trescott, Pinder, and Larson (1976) model was used with several alterations in data output formats. The model uses the implicit finite-difference approximation to the ground-water flow equation. A sparse matrix inversion method known as the strongly implicit procedure was used to solve the approximating equations.

The variables P, E_1, E_2, R, r, D, I, and F are defined briefly by the explanation in figure 3. They are defined more rigorously by their association with the various water flow routes of figure 3. P is the total amount of precipitation that falls into the dashed box. Strictly speaking, it is all water passing into that part of the dashed box which is above ground surface. If water comes from I or P but evaporates before it touches the ground, or passes into the overburden but evapotranspires before reaching the aquifer, it is labeled E_1. Water lost from the box which has come from the aquifer up through the overburden and then evapotranspired is denoted by E_2. Water going into the stream from the overburden but which has not come from the aquifer is small and included in r. Note that r, which is mostly surface runoff, passes into the stream before leaving the box. Thus ideally the box should intersect surface-water drainage divides at land surface. It is assumed that the flow of water from the box and through the overburden is very small and can be ignored. Aquifer water that discharges through the stream bottom and becomes part of the streamflow is labeled D. Flow I is irrigation water pumped from the aquifer. For the sake of being complete, one could also include the small additional amount of water that is removed from the aquifer for other purposes such as domestic supply. Flow F is water from the aquifer which is leaving the box and going into an adjacent aquifer.

The basic budgetary equation for the aquifer is:

$$I = R - (F) - (D + E_2) \qquad (L^3/T). \tag{1}$$

For model area A, when I is zero, equation (1) becomes

$$0.0 = 0.8 - (-0.1) - (0.9) \qquad (\text{in/yr}).$$

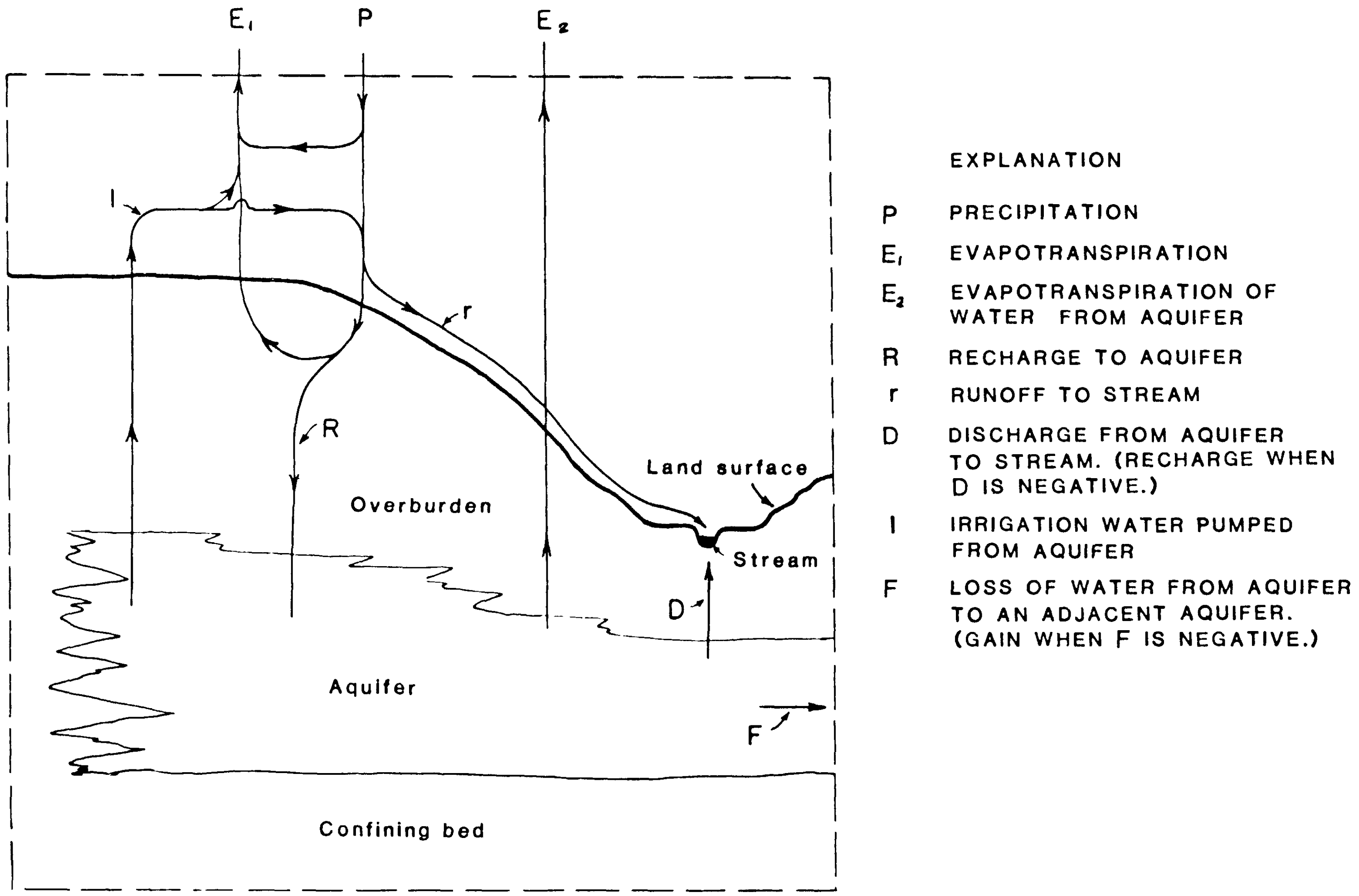

Figure 3.--Total hydrologic system.

When I is not zero, equation (1) becomes

$$0.3 = 0.8 - (-0.1) - (0.6) \qquad \text{(in/yr)}.$$

For the routing of precipitation and irrigation water into runoff r, evapotranspiration E_1, or recharge R:

$$P + I = r + E_1 + R \qquad (L^3/T). \tag{2}$$

For area A, when I is zero, equation (2) becomes

$$18.8 + 0.0 = 0.5 + 17.5 + 0.8 \qquad \text{(in/yr)}.$$

When I is not zero, equation (2) becomes

$$18.8 + 0.3 = 0.5 + 17.8 + 0.8 \qquad \text{(in/yr)}.$$

For model area B: P, R, and r are the same but F is 0.0 in/yr; and $(D + E_2)$ is 0.8 in/yr when I = 0 and 0.0 in/yr when I = 0.8 in/yr. These numerical equations express flow in inches of water per year. When multiplied by the area of the aquifer, they give the amount of water flowing in an average one-year period. Precipitation P is obtained from recorded data and is an average for many years of record, as is runoff r, which is obtained from data on streamflow (r + D), and using $D \ll r$. Irrigation I is known and in the equations above corresponds to the application rate in the area of the aquifer during the year 1978. Recharge R, F, and $(D + E_2)$ of (1) are all obtained from steady-state model solutions to be discussed later, and could have appreciable error. Using this value for R, (2) can be used to find E_1. Note that R is the same with irrigation as without.

Conservation of water in the box gives:

$$P = r + E_1 + F + (D + E_2) \qquad (L^3/T). \tag{3}$$

None of these equations consider the storage of water and thus apply to steady-state situations only. Nevertheless, they should illuminate considerably the basic mechanisms of the total hydrologic system as depicted by figure 3. Appendices I and II give considerably more information on the budgetary details of this system. The notation used in the appendices is somewhat more elaborate; equations (1), (2), and (3) above correspond to equations (4), (5), and (6) in appendix 1.

For time varying situations (1) becomes

$$I = R - (F) - (D + E_2) - \Delta S/\Delta t \qquad (L^3/T). \tag{4}$$

where $\Delta S/\Delta t$ denotes the time rate of change of the amount of water in storage. In the aquifer model of Trescott, Pinder, and Larson (1976), recharge rate R_i, at node i, was assumed to vary with season and i, but to be independent of all other factors (ΔR is zero in appendices I and II). Discharge to streamflow $(D)_i$ from the aquifer in node i varies linearly with the hydraulic head h_i, and is zero when h_i is equal to the elevation of the stream in the node. $(D)_i$ is negative when h_i is below the stream elevation. Evapotranspiration from node i, $(E_2)_i$, also varies linearly with the hydraulic head h_i at node i but is zero when h_i is a distance b_i or greater below land surface. The model determines the terms F, $D + E_2 = \Sigma(D + E_2)_i$, and $\Delta S/\Delta t$ in aquifer budget equation (4), as well as the hydraulic head h_i at each node i. The other terms in (4), $I = \Sigma I_i$ and $R = \Sigma R_i$, are parameters for the numerical solution carried out by the model. The I_i are taken from irrigation data and are thus known functions of time. Parameters of the numerical solution which are not known completely are: The R_i which are time dependent, the quantities b_i, the rate of increase of $(D + E_2)_i$ with h_i, the hydraulic conductivities k_i, and also either or both of the specific yield $(S_y)_i$ or storage coefficient S_i at each node i. These parameters are adjusted to calibrate the model.

Except for nodes along the James River, discharge to streamflow $(D)_i$ was assumed to be zero. All the nodes along the river have an evapotranspiration $(E_2)_i$ greater than zero, even when the aquifer is stressed by irrigation pumpage which usually occurs at some distance from the river. Because of this situation, the aquifer model cannot distinguish between $(D)_i$ and $(E_2)_i$ for the nodes along the river so that only the lumped value $(D + E_2)_i$ is determined.

Model Calibration

Calibration is that process by which a model is altered and the parameters of the model adjusted so that it can best simulate certain variables of a physical system. In this study, these variables were the hydraulic heads h_i at those nodes i of the aquifer model where observation-well data existed. In model areas A and B of figure 2, 108 and 58 nodes respectively had measured observation well data for h_i, usually as a function of time. Aquifer discharge D to streamflow, present as measured data in many studies and of considerable value to the calibration procedure, was too small to measure in this study. Estimates of evaporation E_2 from increased crop yield are very inaccurate and therefore of limited use for improving calibration.

Figure 3 was taken as a suitable conceptualization of the total hydrologic system. The budgetary equations (1)-(4), as well as those in the appendices, were used as an additional framework or conceptualization of the total hydrologic system. In addition, the recharge rate R_i into node i was assumed to be independent of all factors except time and node number i. $(S_y)_i$ and S_i were assumed to be the same for all i. The locations along the aquifer perimeter where F was allowed to be non-zero are shown in figure 2 adjacent to the constant head symbol ▿. As mentioned previously, discharge to streamflow D was assumed to be zero for all streams except the James River.

The aquifer was modeled as two areas (see fig. 2), called model areas A and B, for the convenience of data output. Certain nodes along the James River where the two model areas join were shared by both model areas A and B. At these nodes, values for hydraulic head h calculated were approximately the same for the two model areas. This head match was accomplished by choosing the same b_i and rates of increase of $(D + E_2)_i$ with h_i, at the river nodes where the model areas join.

The major part of the calibration consisted of varying the parameters $R_i(t)$ where t denotes time, b_i, the rate of increase of $(D + E_2)_i$ with h_i, k_i, $(S_y)_i$, and S_i, in such a manner that the goodness of fit of the hydraulic heads $h_i(t)$, produced as dependent variables by the model, with the measured hydraulic heads $h_i(t)$ was maximized. For steady-state calibration, corresponding to steady-state flow, with R_i constant in time and $I_i = 0$, this was done by adjusting the above parameters such that the standard error of estimate

$$S_{err} = \left(\sum_{i=1}^{N} w_i(h_i - h_i)^2 / \sum_{i=1}^{N} w_i \right)^{1/2} \qquad (5)$$

was minimized. The summation in (5) is over those nodes having a measured hydraulic head $\hat{h}_i$ only. N was 108 and 58 for model areas A and B respectively, which were calibrated separately. The w_i are weights and were given the value 1.0 when $\hat{h}_i$ was considered to be completely reliable, and 0.5 when less than completely reliable. Time-dependent calibrations, with R_i and I_i functions of time t, were done by matching $h_i(t)$ with $\hat{h}_i(t)$ at time intervals Δt equal to (365/12) days and 365 days. During each time interval Δt, $R_i(t)$ and $I_i(t) \neq 0$ were equal to their time averaged constant values.

The parameter estimation procedure described above is in effect a trial-and-error adjustment of the parameters so as to increase the goodness of fit of, in this case, $h_i(t)$ with $\hat{h}_i(t)$. In the general trial-and-error approach, the modeler continually adjusts the parameters on the basis of a variety of notions or possible misconceptions that he has about the aquifer. Consequently, the trial-and-error approach is in general very subjective. Steady-state calibrations with $I = 0$, using pre-irrigation $\hat{h}_i$ data, are poor because if R_i, the rate of increase of $(D + E_2)_i$ with h_i, and k_i, are all multiplied by the same factor, the model gives the same h_i. At present, irrigation effects are still in an early stage and equilibrium, if possible, is still many years away, thus steady-state calibrations are not possible with $I \neq 0$ because there is no data for $\hat{h}_i$. Time-dependent calibrations tend to be heavily involved with the selection of $(S_y)_i$, S_i, and the time dependence of $R_i(t)$, at the expense of the estimation of the other parameters. Nevertheless, it is the author's belief that a fairly reasonable calibration has been achieved considering the difficult circumstances.

Model Input

Certain inputs into the model are known from measurement. These are: Land surface altitude and the altitude of the top and bottom of the aquifer, irrigation pumpage $I_i(t)$, and the measured hydraulic heads $\hat{h}_i(t)$ at each node i.

Figures 4 and 5 show land surface altitude in feet, above a datum of 1,000 ft above sea level, for aquifer model areas A and B. Figures 6 and 7 show aquifer top altitude, again above a datum of 1,000 ft above sea level. Figures 8 and 9 show aquifer bottom altitude. As explained previously, aquifer top and bottom altitudes, for a particular node, were obtained by taking the average of aquifer top and bottom altitudes from drill hole data in that node. When a node did not have any drill hole data, aquifer top and bottom altitudes were extrapolated from nearby nodes having such data. Figures 10 and 11 show the thickness of the aquifer. The row and column node numbers are along the left and top of each figure. Land surface elevations, figures 4 and 5, are used by the aquifer model to determine the evapotranspiration $(E_2)_i$ from each node i. $(E_2)_i$ varies linearly with hydraulic head h_i and is zero when h_i is at a distance b_i or greater below land surface. In some cases, a large low-lying land surface over part of a node has sufficient area to allow significant amounts of evapotranspiration $(E_2)_i$, but the aquifer top elevation for the node, perhaps obtained from data at a high altitude point within the node, is at an altitude that is above this land surface. For such a node, the aquifer top elevation, figures 6 and 7, would be at a higher altitude than the land surface elevation in figures 4 and 5. A few nodes in the model have low-lying land surface areas for evapotranspiration but, according to available drill-hole data, both the aquifer top and bottom are above the altitude of this land surface. This situation is shown in figure 12, which depicts a single 1-mi^2 node from a side view. In the model, when h_i shown was greater than the aquifer bottom elevation, the transmissivity of the node was set equal to the hydraulic conductivity of the node k_i multiplied by the saturated thickness in the usual manner. However, when h_i fell below the aquifer bottom elevation, the transmissivity was not set to zero but was instead set

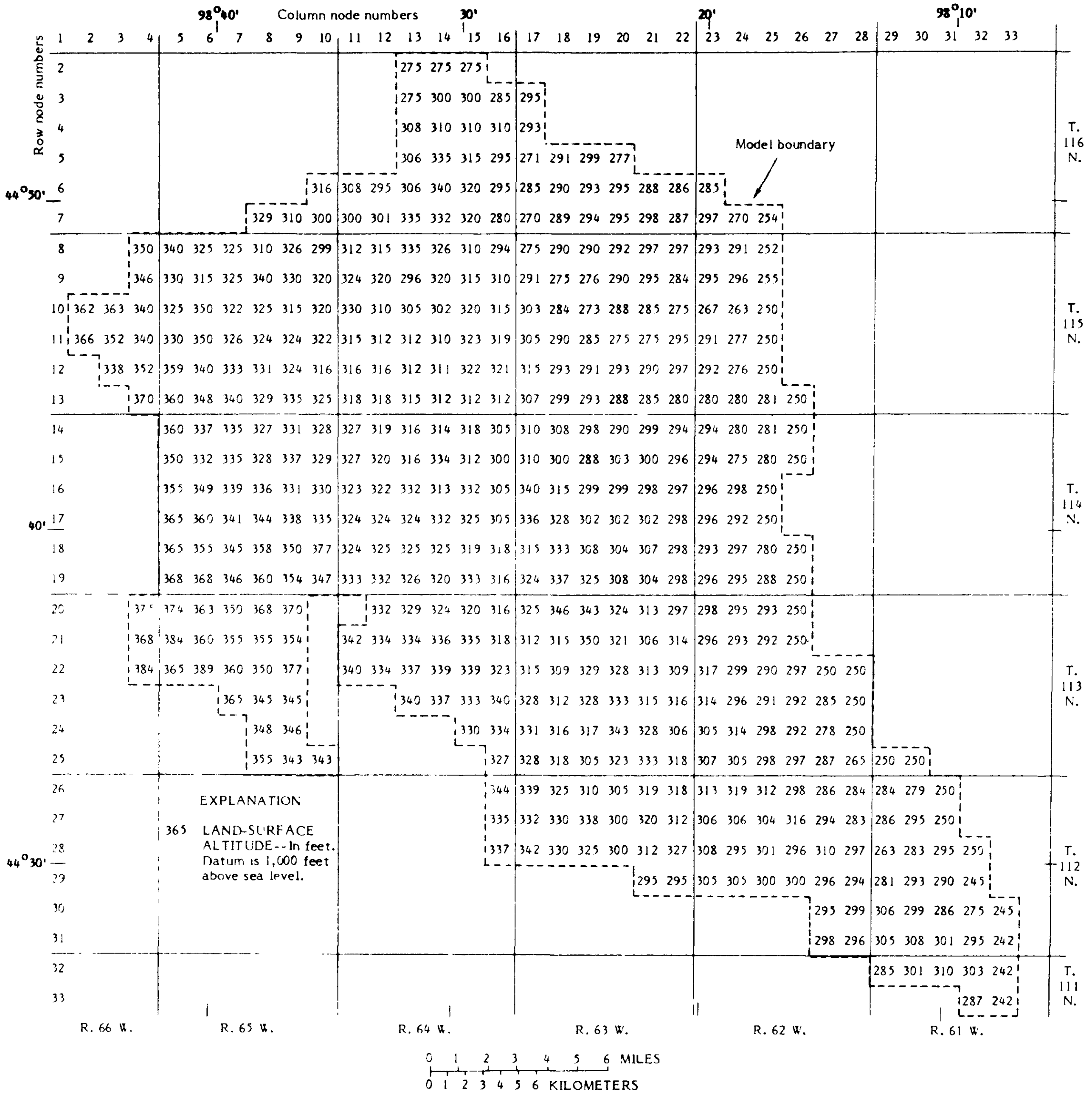

EXPLANATION

365 LAND-SURFACE ALTITUDE--In feet. Datum is 1,000 feet above sea level.

	1	2	3	4	5	6	7	8	9	10	11	12	13	14	15	16	17	18	19	20	21	22	23	24	25	26	27	28	29	30	31	32	33
2													275	275	275																		
3													275	300	300	285	295																
4													308	310	310	310	293																
5													306	335	315	295	271	291	299	277													
6										316	308	295	306	340	320	295	285	290	293	295	288	286	285										
7								329	310	300	300	301	335	332	320	280	270	289	294	295	298	287	297	270	254								
8				350	340	325	325	310	326	299	312	315	335	326	310	294	275	290	290	292	297	297	293	291	252								
9				346	330	315	325	340	330	320	324	320	296	320	315	310	291	275	276	290	295	284	295	296	255								
10		362	363	340	325	350	322	325	315	320	330	310	305	302	320	315	303	284	273	288	285	275	267	263	250								
11		366	352	340	330	350	326	324	324	322	315	312	312	310	323	319	305	290	285	275	275	295	291	277	250								
12			338	352	359	340	333	331	324	316	316	316	312	311	322	321	315	293	291	293	290	297	292	276	250								
13				370	360	348	340	329	335	325	318	318	315	312	312	312	307	299	293	288	285	280	280	280	281	250							
14					360	337	335	327	331	328	327	319	316	314	318	305	310	308	298	290	299	294	294	280	281	250							
15					350	332	335	328	337	329	327	320	316	334	312	300	310	300	288	303	300	296	294	275	280	250							
16					355	349	339	336	331	330	323	322	332	313	332	305	340	315	299	299	298	297	296	298	250								
17					365	360	341	344	338	335	324	324	324	332	325	305	336	328	302	302	302	298	296	292	250								
18					365	355	345	358	350	377	324	325	325	325	319	318	315	333	308	304	307	298	293	297	780	250							
19					368	368	346	360	354	347	333	332	326	320	333	316	324	337	325	308	304	298	296	295	288	250							
20				375	374	363	350	368	370			332	329	324	320	316	325	346	343	324	313	297	298	295	293	250							
21				368	384	360	355	355	354		342	334	334	336	335	318	312	315	350	321	306	314	296	293	292	250							
22				384	365	389	360	350	377		340	334	337	339	339	323	315	309	329	328	313	309	317	299	290	297	250	250					
23							365	345	345				340	337	333	340	328	312	328	333	315	316	314	296	291	292	285	250					
24								348	346						330	334	331	316	317	343	328	306	305	314	298	292	278	250					
25								355	343	343						327	328	318	305	323	333	318	307	305	298	297	287	265	250	250			
26																344	339	325	310	305	319	318	313	319	312	298	286	284	284	279	250		
27																335	332	330	338	300	320	312	306	306	304	316	294	283	286	295	250		
28																337	342	330	325	300	312	327	308	295	301	296	310	297	263	283	295	250	
29																					295	295	305	305	300	300	296	294	281	293	290	245	
30																											295	299	306	299	286	275	245
31																											298	296	305	308	301	295	242
32																													285	301	310	303	242
33																																287	242

Figure 4.--Altitude of land surface in model area A.

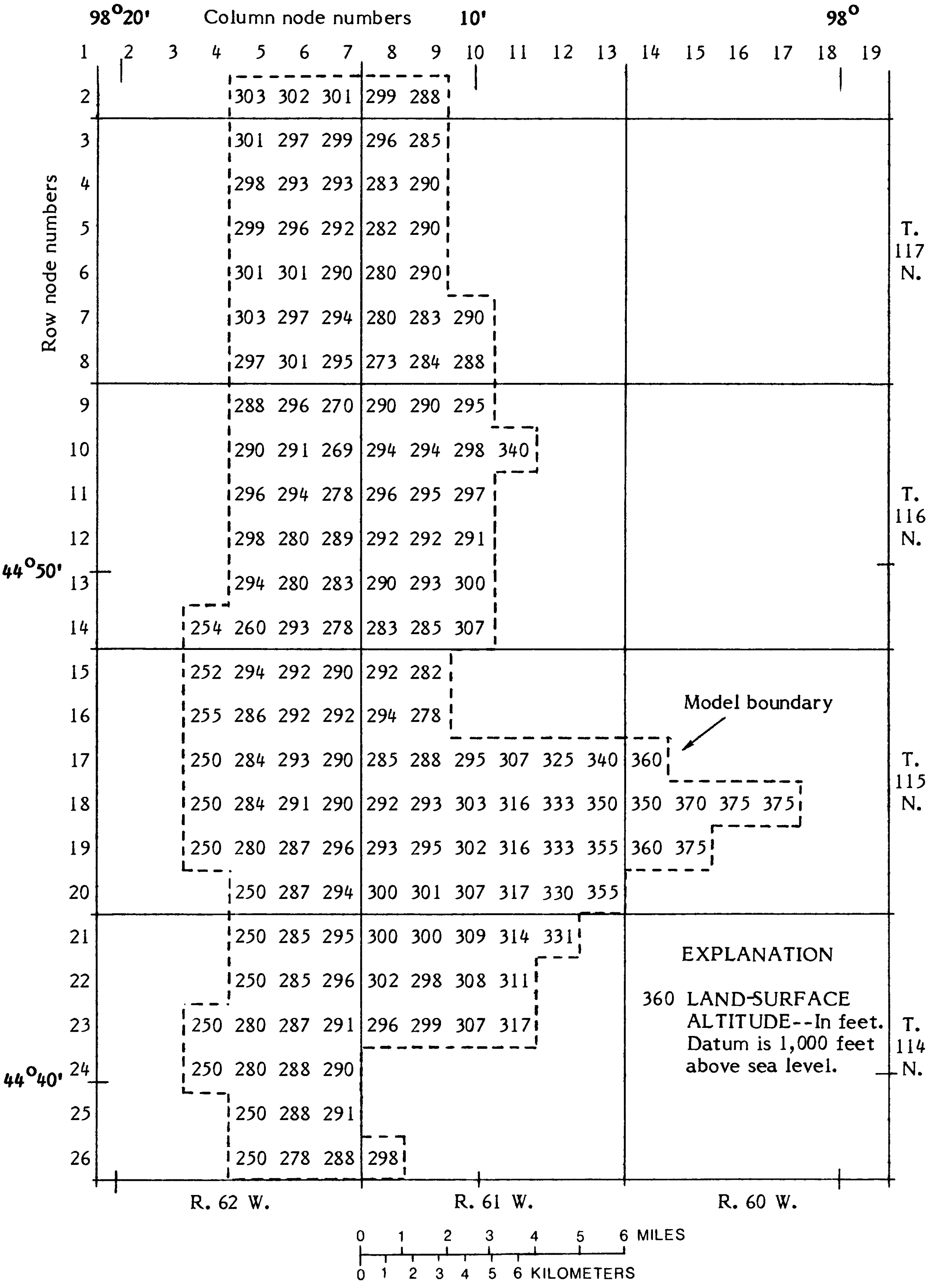

	1	2	3	4	5	6	7	8	9	10	11	12	13	14	15	16	17	18	19
2					303	302	301	299	288										
3					301	297	299	296	285										
4					298	293	293	283	290										
5					299	296	292	282	290										
6					301	301	290	280	290										
7					303	297	294	280	283	290									
8					297	301	295	273	284	288									
9					288	296	270	290	290	295									
10					290	291	269	294	294	298	340								
11					296	294	278	296	295	297									
12					298	280	289	292	292	291									
13					294	280	283	290	293	300									
14				254	260	293	278	283	285	307									
15				252	294	292	290	292	282										
16				255	286	292	292	294	278										
17				250	284	293	290	285	288	295	307	325	340	360					
18				250	284	291	290	292	293	303	316	333	350	350	370	375	375		
19				250	280	287	296	293	295	302	316	333	355	360	375				
20					250	287	294	300	301	307	317	330	355						
21					250	285	295	300	300	309	314	331							
22					250	285	296	302	298	308	311								
23				250	280	287	291	296	299	307	317								
24				250	280	288	290												
25					250	288	291												
26					250	278	288	298											

Figure 5.--Altitude of land surface in model area B.

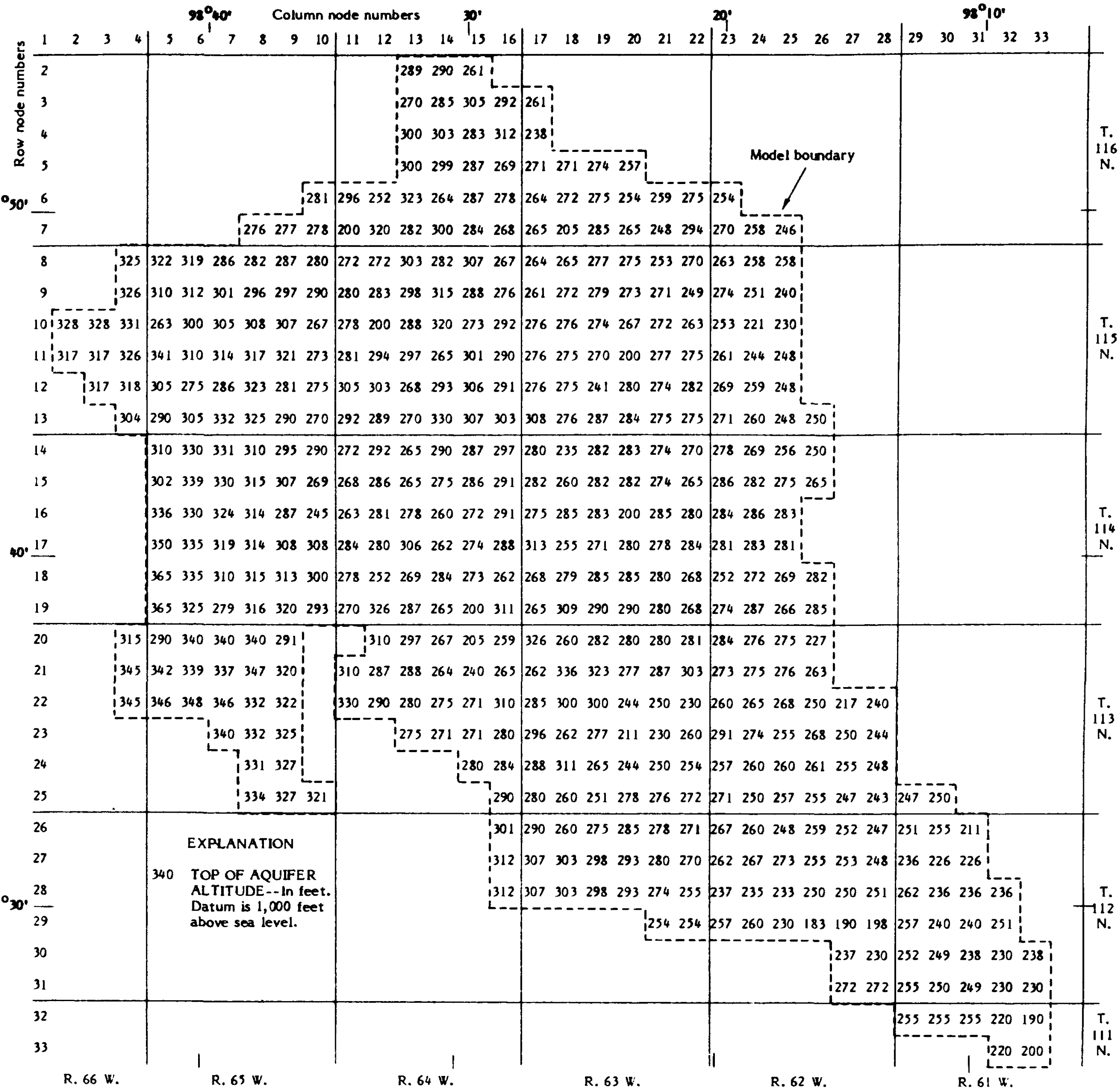

Row node numbers	1	2	3	4	5	6	7	8	9	10	11	12	13	14	15	16	17	18	19	20	21	22	23	24	25	26	27	28	29	30	31	32	33
2													289	290	261																		
3													270	285	305	292	261																
4													300	303	283	312	238																
5													300	299	287	269	271	271	274	257													
6										281	296	252	323	264	287	278	264	272	275	254	259	275	254										
7								276	277	278	200	320	282	300	284	268	265	205	285	265	248	294	270	258	246								
8				325	322	319	286	282	287	280	272	272	303	282	307	267	264	265	277	275	253	270	263	258	258								
9				326	310	312	301	296	297	290	280	283	298	315	288	276	261	272	279	273	271	249	274	251	240								
10		328	328	331	263	300	305	308	307	267	278	200	288	320	273	292	276	276	274	267	272	263	253	221	230								
11		317	317	326	341	310	314	317	321	273	281	294	297	265	301	290	276	275	270	200	277	275	261	244	248								
12			317	318	305	275	286	323	281	275	305	303	268	293	306	291	276	275	241	280	274	282	269	259	248								
13				304	290	305	332	325	290	270	292	289	270	330	307	303	308	276	287	284	275	275	271	260	248	250							
14					310	330	331	310	295	290	272	292	265	290	287	297	280	235	282	283	274	270	278	269	256	250							
15					302	339	330	315	307	269	268	286	265	275	286	291	282	260	282	282	274	265	286	282	275	265							
16					336	330	324	314	287	245	263	281	278	260	272	291	275	285	283	200	285	280	284	286	283								
17					350	335	319	314	308	308	284	280	306	262	274	288	313	255	271	280	278	284	281	283	281								
18					365	335	310	315	313	300	278	252	269	284	273	262	268	279	285	285	280	268	252	272	269	282							
19					365	325	279	316	320	293	270	326	287	265	200	311	265	309	290	290	280	268	274	287	266	285							
20				315	290	340	340	340	291			310	297	267	205	259	326	260	282	280	280	281	284	276	275	227							
21				345	342	339	337	347	320		310	287	288	264	240	265	262	336	323	277	287	303	273	275	276	263							
22				345	346	348	346	332	322		330	290	280	275	271	310	285	300	300	244	250	230	260	265	268	250	217	240					
23							340	332	325				275	271	271	280	296	262	277	211	230	260	291	274	255	268	250	244					
24								331	327						280	284	288	311	265	244	250	254	257	260	260	261	255	248					
25								334	327	321						290	280	260	251	278	276	272	271	250	257	255	247	243	247	250			
26																301	290	260	275	285	278	271	267	260	248	259	252	247	251	255	211		
27																312	307	303	298	293	280	270	262	267	273	255	253	248	236	226	226		
28																312	307	303	298	293	274	255	237	235	233	250	250	251	262	236	236	236	
29																					254	254	257	260	230	183	190	198	257	240	240	251	
30																											237	230	252	249	238	230	238
31																											272	272	255	250	249	230	230
32																													255	255	255	220	190
33																																220	200

Figure 6.--Altitude of top of aquifer in model area A.

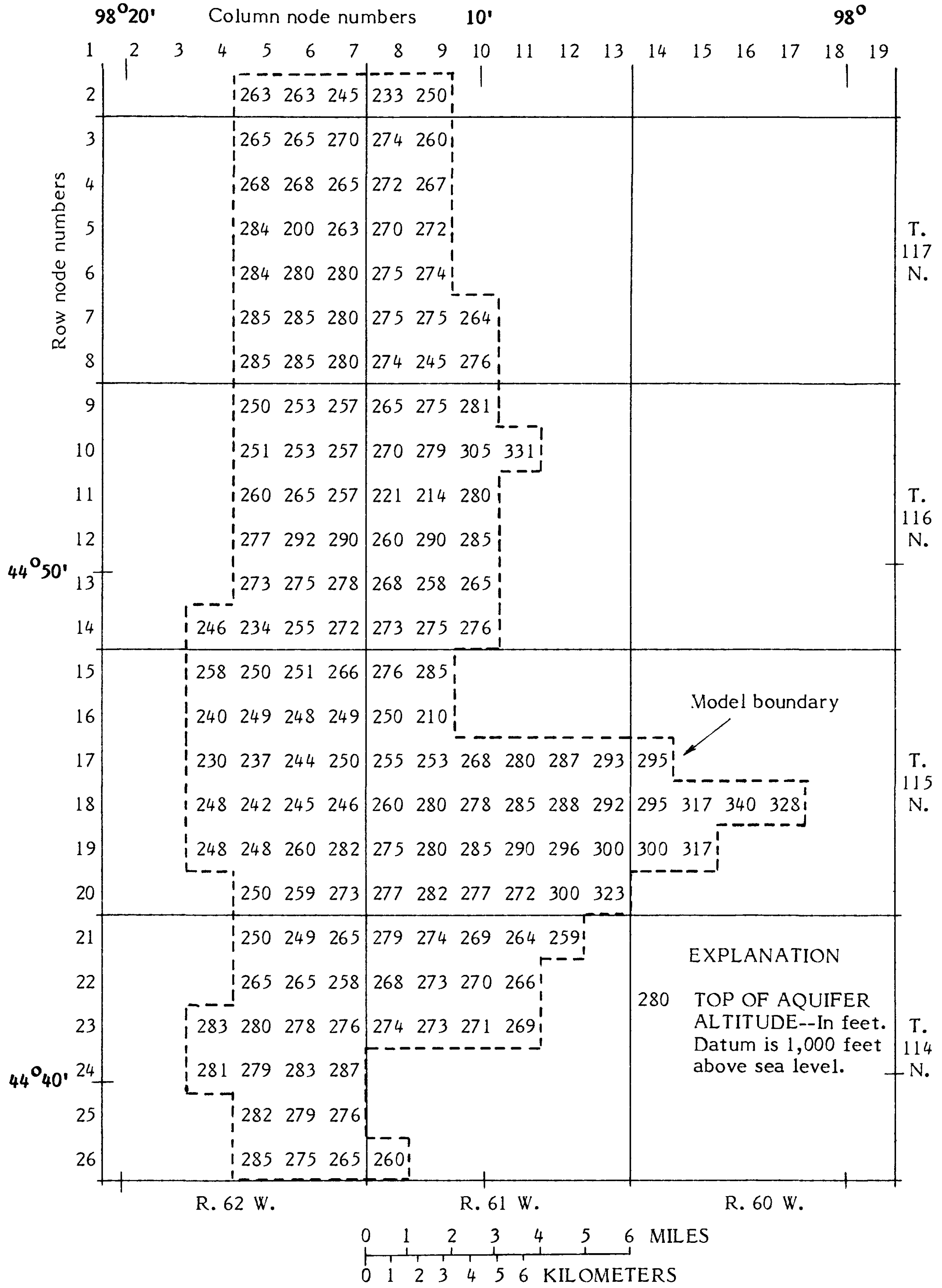

	1	2	3	4	5	6	7	8	9	10	11	12	13	14	15	16	17	18	19
2					263	263	245	233	250										
3					265	265	270	274	260										
4					268	268	265	272	267										
5					284	200	263	270	272										
6					284	280	280	275	274										
7					285	285	280	275	275	264									
8					285	285	280	274	245	276									
9					250	253	257	265	275	281									
10					251	253	257	270	279	305	331								
11					260	265	257	221	214	280									
12					277	292	290	260	290	285									
13					273	275	278	268	258	265									
14				246	234	255	272	273	275	276									
15				258	250	251	266	276	285										
16				240	249	248	249	250	210										
17				230	237	244	250	255	253	268	280	287	293	295					
18				248	242	245	246	260	280	278	285	288	292	295	317	340	328		
19				248	248	260	282	275	280	285	290	296	300	300	317				
20					250	259	273	277	282	277	272	300	323						
21					250	249	265	279	274	269	264	259							
22					265	265	258	268	273	270	266								
23				283	280	278	276	274	273	271	269								
24				281	279	283	287												
25					282	279	276												
26					285	275	265	260											

EXPLANATION

280 TOP OF AQUIFER ALTITUDE--In feet. Datum is 1,000 feet above sea level.

Figure 7.--Altitude of top of aquifer in model area B.

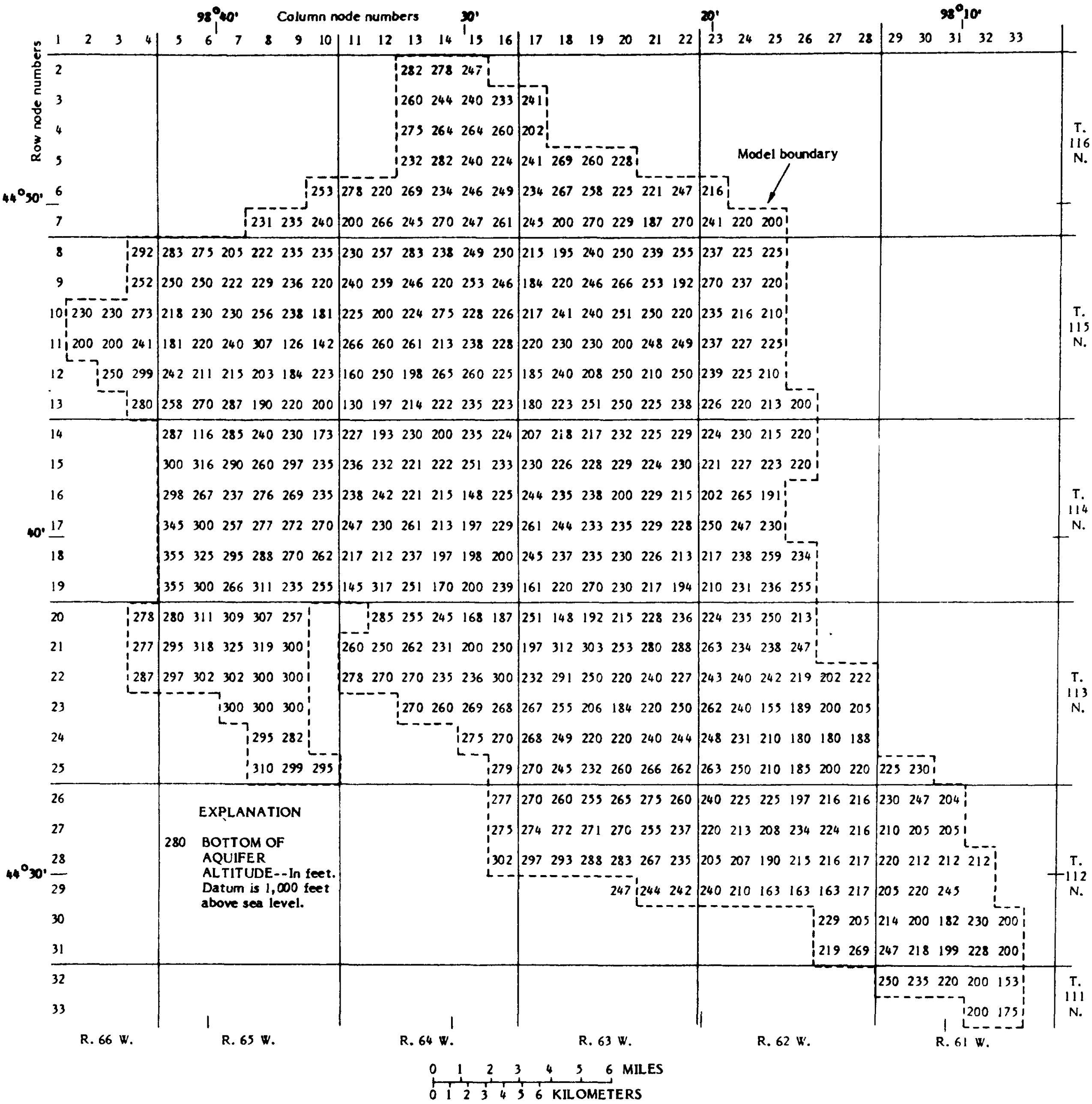

Figure 8.--Altitude of bottom of aquifer in model area A.

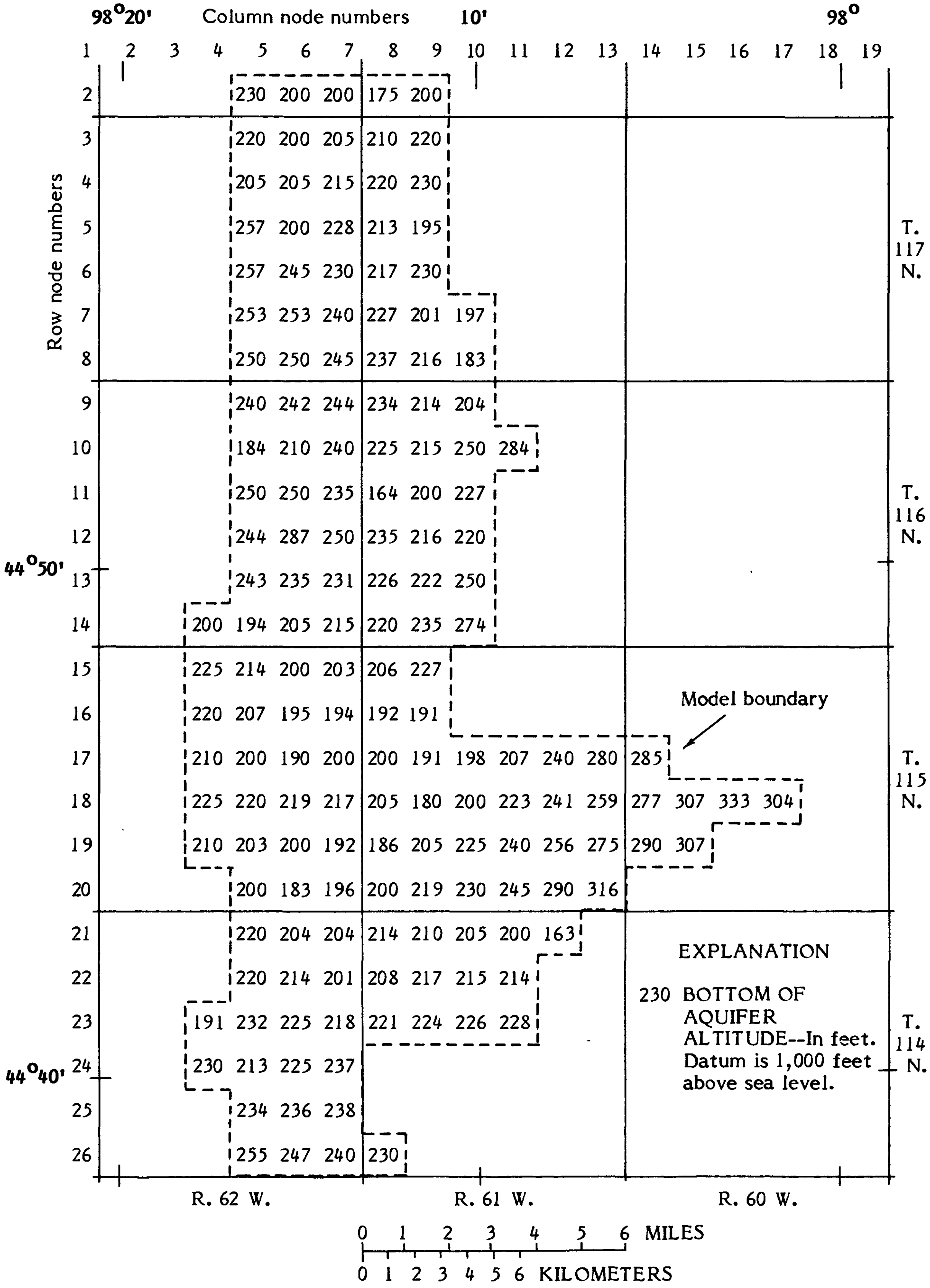

	1	2	3	4	5	6	7	8	9	10	11	12	13	14	15	16	17	18	19
2					230	200	200	175	200										
3					220	200	205	210	220										
4					205	205	215	220	230										
5					257	200	228	213	195										
6					257	245	230	217	230										
7					253	253	240	227	201	197									
8					250	250	245	237	216	183									
9					240	242	244	234	214	204									
10					184	210	240	225	215	250	284								
11					250	250	235	164	200	227									
12					244	287	250	235	216	220									
13					243	235	231	226	222	250									
14				200	194	205	215	220	235	274									
15				225	214	200	203	206	227										
16				220	207	195	194	192	191										
17				210	200	190	200	200	191	198	207	240	280	285					
18				225	220	219	217	205	180	200	223	241	259	277	307	333	304		
19				210	203	200	192	186	205	225	240	256	275	290	307				
20					200	183	196	200	219	230	245	290	316						
21					220	204	204	214	210	205	200	163							
22					220	214	201	208	217	215	214								
23				191	232	225	218	221	224	226	228								
24				230	213	225	237												
25					234	236	238												
26					255	247	240	230											

EXPLANATION

230 BOTTOM OF AQUIFER ALTITUDE--In feet. Datum is 1,000 feet above sea level.

Figure 9.--Altitude of bottom of aquifer in model area B.

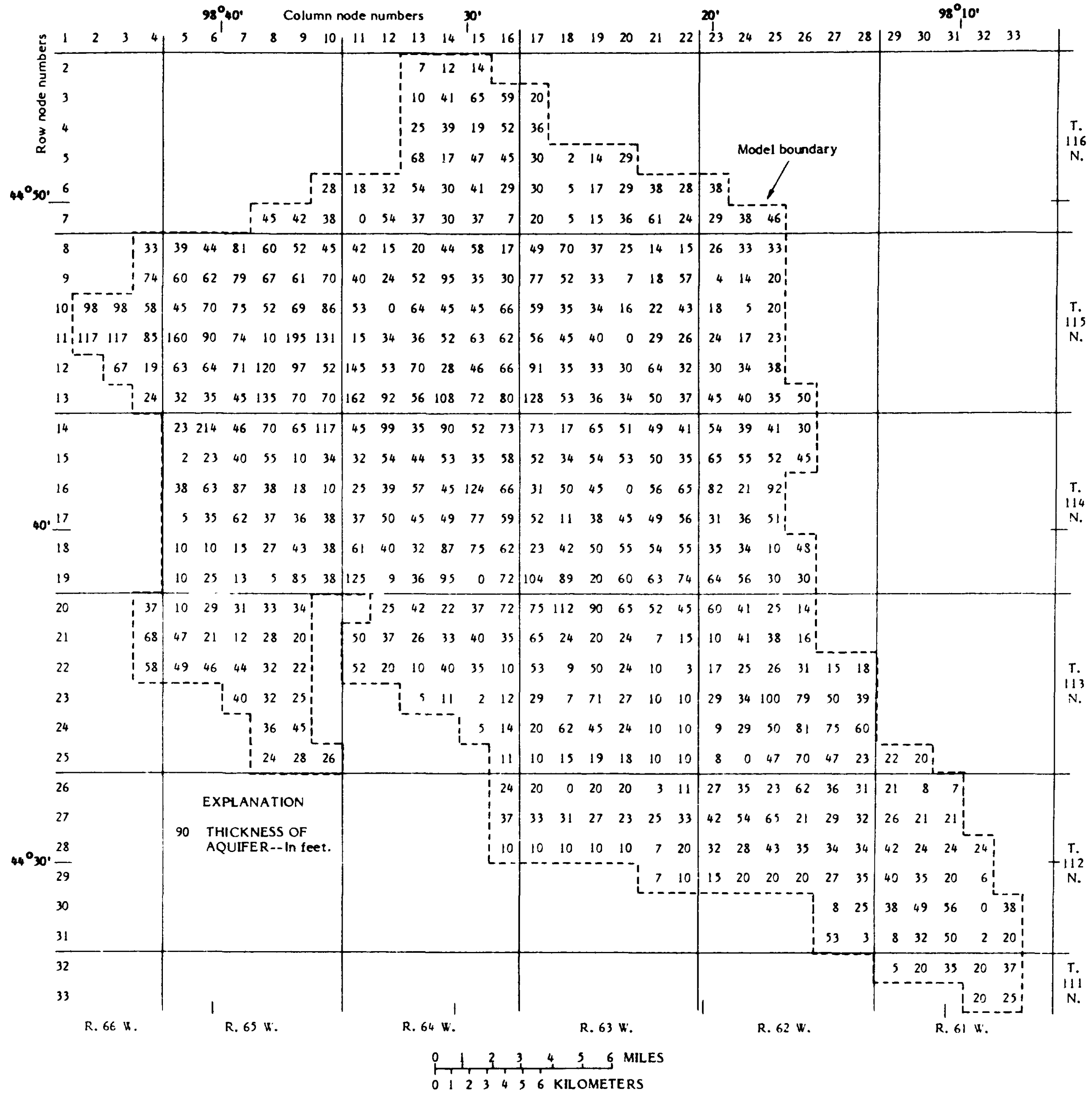

Row node numbers	1	2	3	4	5	6	7	8	9	10	11	12	13	14	15	16	17	18	19	20	21	22	23	24	25	26	27	28	29	30	31	32	33
2													7	12	14																		
3													10	41	65	59	20																
4													25	39	19	52	36																
5													68	17	47	45	30	2	14	29													
6										28	18	32	54	30	41	29	30	5	17	29	38	28	38										
7								45	42	38	0	54	37	30	37	7	20	5	15	36	61	24	29	38	46								
8				33	39	44	81	60	52	45	42	15	20	44	58	17	49	70	37	25	14	15	26	33	33								
9				74	60	62	79	67	61	70	40	24	52	95	35	30	77	52	33	7	18	57	4	14	20								
10		98	98	58	45	70	75	52	69	86	53	0	64	45	45	66	59	35	34	16	22	43	18	5	20								
11		117	117	85	160	90	74	10	195	131	15	34	36	52	63	62	56	45	40	0	29	26	24	17	23								
12			67	19	63	64	71	120	97	52	145	53	70	28	46	66	91	35	33	30	64	32	30	34	38								
13				24	32	35	45	135	70	70	162	92	56	108	72	80	128	53	36	34	50	37	45	40	35	50							
14					23	214	46	70	65	117	45	99	35	90	52	73	73	17	65	51	49	41	54	39	41	30							
15					2	23	40	55	10	34	32	54	44	53	35	58	52	34	54	53	50	35	65	55	52	45							
16					38	63	87	38	18	10	25	39	57	45	124	66	31	50	45	0	56	65	82	21	92								
17					5	35	62	37	36	38	37	50	45	49	77	59	52	11	38	45	49	56	31	36	51								
18					10	10	15	27	43	38	61	40	32	87	75	62	23	42	50	55	54	55	35	34	10	48							
19					10	25	13	5	85	38	125	9	36	95	0	72	104	89	20	60	63	74	64	56	30	30							
20				37	10	29	31	33	34			25	42	22	37	72	75	112	90	65	52	45	60	41	25	14							
21				68	47	21	12	28	20		50	37	26	33	40	35	65	24	20	24	7	15	10	41	38	16							
22				58	49	46	44	32	22		52	20	10	40	35	10	53	9	50	24	10	3	17	25	26	31	15	18					
23							40	32	25				5	11	2	12	29	7	71	27	10	10	29	34	100	79	50	39					
24								36	45						5	14	20	62	45	24	10	10	9	29	50	81	75	60					
25								24	28	26						11	10	15	19	18	10	10	8	0	47	70	47	23	22	20			
26																24	20	0	20	20	3	11	27	35	23	62	36	31	21	8	7		
27																37	33	31	27	23	25	33	42	54	65	21	29	32	26	21	21		
28																10	10	10	10	10	7	20	32	28	43	35	34	34	42	24	24	24	
29																					7	10	15	20	20	20	27	35	40	35	20	6	
30																											8	25	38	49	56	0	38
31																											53	3	8	32	50	2	20
32																													5	20	35	20	37
33																																20	25

Figure 10.--Thickness of aquifer in model area A.

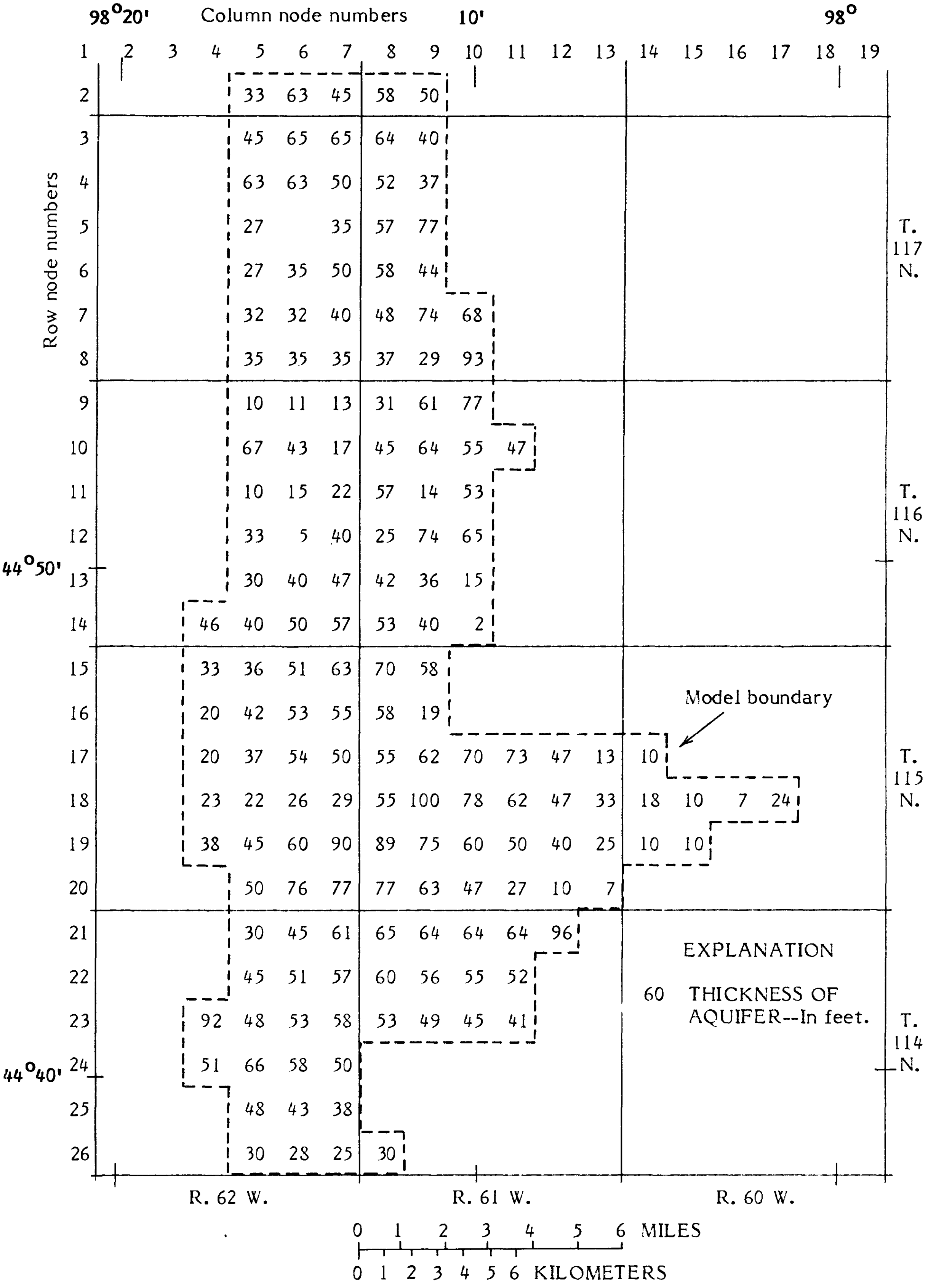

	4	5	6	7	8	9	10	11	12	13	14	15	16	17
2		33	63	45	58	50								
3		45	65	65	64	40								
4		63	63	50	52	37								
5		27		35	57	77								
6		27	35	50	58	44								
7		32	32	40	48	74	68							
8		35	35	35	37	29	93							
9		10	11	13	31	61	77							
10		67	43	17	45	64	55	47						
11		10	15	22	57	14	53							
12		33	5	40	25	74	65							
13		30	40	47	42	36	15							
14	46	40	50	57	53	40	2							
15	33	36	51	63	70	58								
16	20	42	53	55	58	19								
17	20	37	54	50	55	62	70	73	47	13	10			
18	23	22	26	29	55	100	78	62	47	33	18	10	7	24
19	38	45	60	90	89	75	60	50	40	25	10	10		
20		50	76	77	77	63	47	27	10	7				
21		30	45	61	65	64	64	64	96					
22		45	51	57	60	56	55	52						
23	92	48	53	58	53	49	45	41						
24	51	66	58	50										
25		48	43	38										
26		30	28	25	30									

Figure 11.--Thickness of aquifer in model area B.

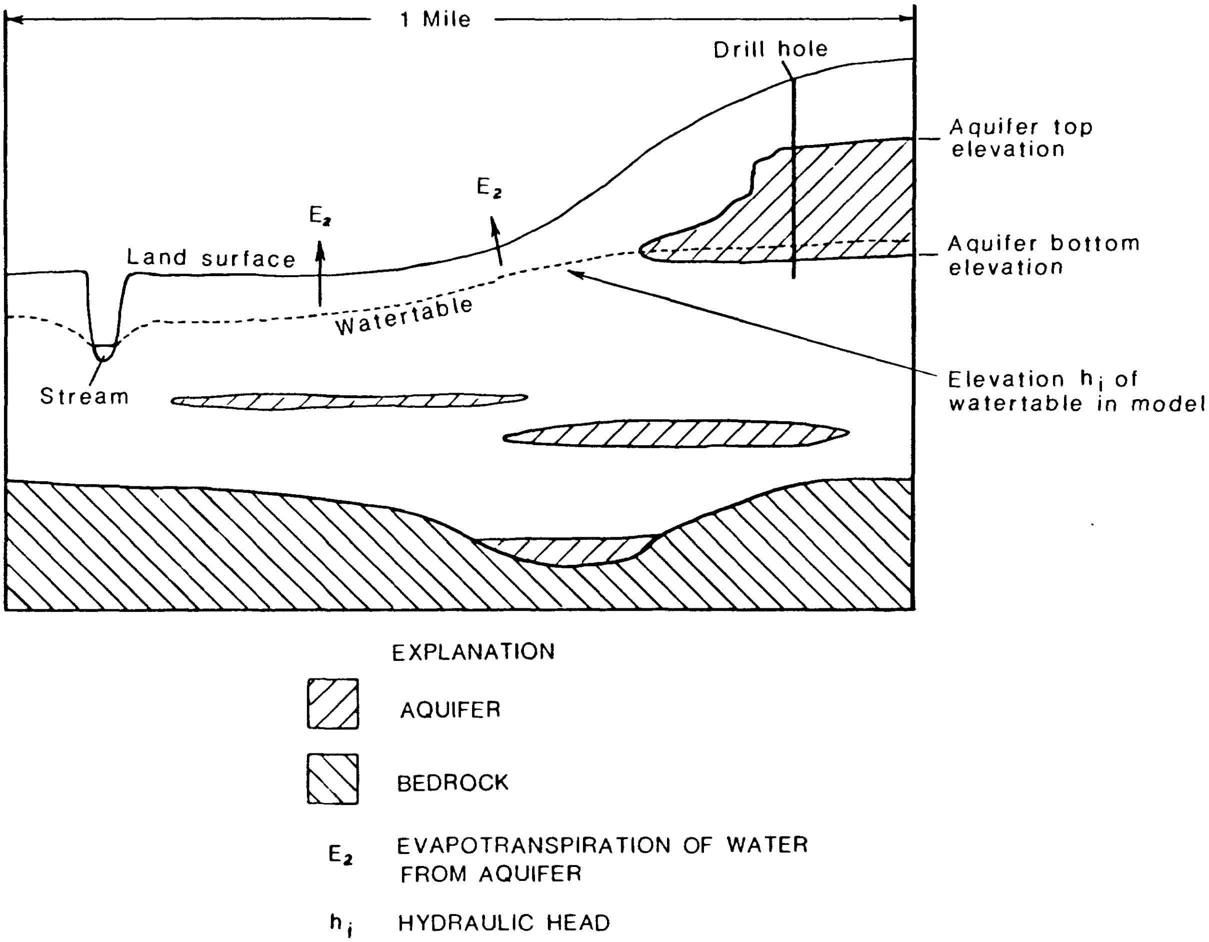

Figure 12.--Model node.

equal to the hydraulic conductivity of the node k_i multiplied by a thickness of 1.0 ft. This prescription for calculating the transmissivity of the nodes may seem somewhat arbitrary, but it should be remembered that the sediments beneath the aquifers do not have zero hydraulic conductivity but rather a non-zero value much lower than the aquifers. Quite likely at depths below the aquifer bottom elevation, one or more additional aquifers may be present. The transmissivity for the node shown in figure 12 will be calculated as 1.0 ft times the hydraulic conductivity k_i for the node. This will give a small value for the transmissivity and will thus properly restrict the flow of water from adjacent nodes before discharging as discharge to streamflow D and evapotranspiration E_2.

Figures 13 and 14 show the reported quantity of water pumped for irrigation I_i during the year 1978. Actual use may have been somewhat larger since, as in other years, not all the irrigators responded to the questionnaires which were sent to them. All hydraulic head data used were for the year 1978 or earlier. Figures 15 and 16 show $\hat{h}_i$, i = 1, N for N = 108 and N = 58, respectively. These $\hat{h}_i$ are time averages of hydraulic head for times prior to the onset of irrigation, when available, but in some cases are time averages of more recent hydraulic head data. Note that some of the nodes along the James River are predominant as sinks for the flow of water, and that the gradient of $\hat{h}$ can be quite large near the river. Observation-well data for 1968-78, an 11-year period of nearly average total rainfall, show that the hydraulic head decreased as much as 2 to 5 ft in some areas of the southeastern part of aquifer area A and the northern part of aquifer area B. In other areas of the aquifer, where observation-well data for 1968-78 was available, hydraulic head usually declined by smaller amounts. These declines are very small compared with the change that occurs in the hydraulic head as one moves horizontally across the aquifer. The $\hat{h}_i$ in figures 15 and 16 were used for steady-state calibration with $I_i = 0$, the R_i constant in time and equal to average yearly recharge rate into node i, and the use of the standard error of estimate in equation (5).

Model Results

Calibration gave estimates for the parameters $R_i(t)$, b_i, the rate of increase of $(D + E_2)_i$ with h_i, k_i, $(S_y)_i$, and S_i, at each node i.

Figures 17 and 18 give the best estimates of the parameters R_i, as determined by all of the calibration used, both steady-state and time-dependent. The recharge rate values shown are in units of 0.1 in/yr and represent yearly recharge rate for an average year. For years of heavy rainfall, recharge increases substantially. In years of drought it may be nearly zero. Figures 19 and 20 give the best estimates for the parameters k_i in units of ft/d, again as determined by both steady-state and time-dependent calibration. The best estimate values for b_i were from 12 to 22 ft. During time-dependent calibration, the $(S_y)_i$ and S_i were varied but were not allowed to vary with i. This would have been necessary if one had tried to simulate the monthly time dependence of each $\hat{h}_i(t)$. This was not done, however, so that only a best estimate for a single S_y and S was obtained. For aquifer areas A and B, these best estimates were 0.20 and 0.008, and 0.20 and 0.012, respectively.

The remainder of this section presents results produced by the aquifer model using the measured inputs and parameter estimations given above, as well as additional parameter estimations related to the time-dependence of $R_i(t)$.

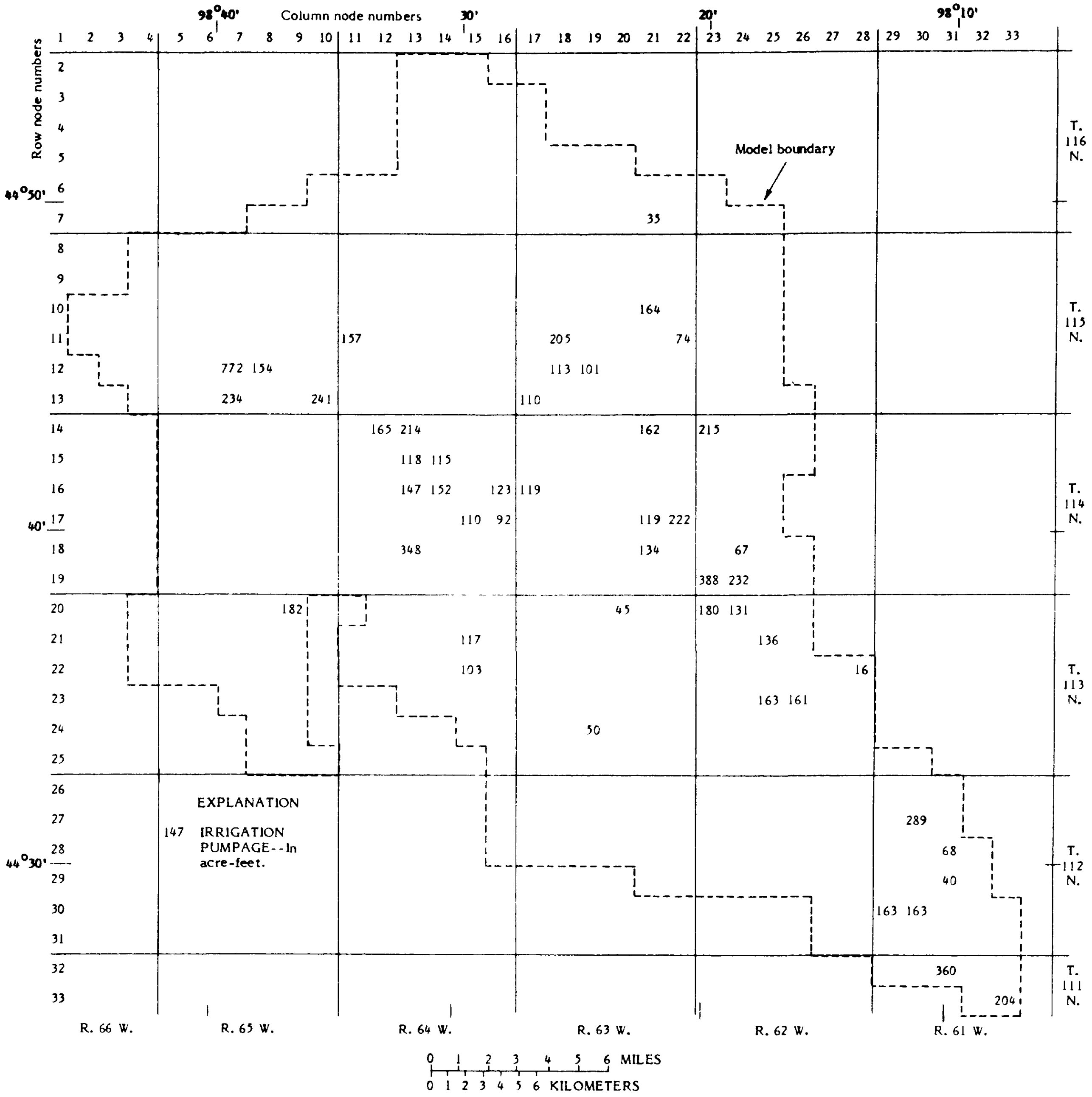

Figure 13.--Reported irrigation pumpage for 1978 in model area A.

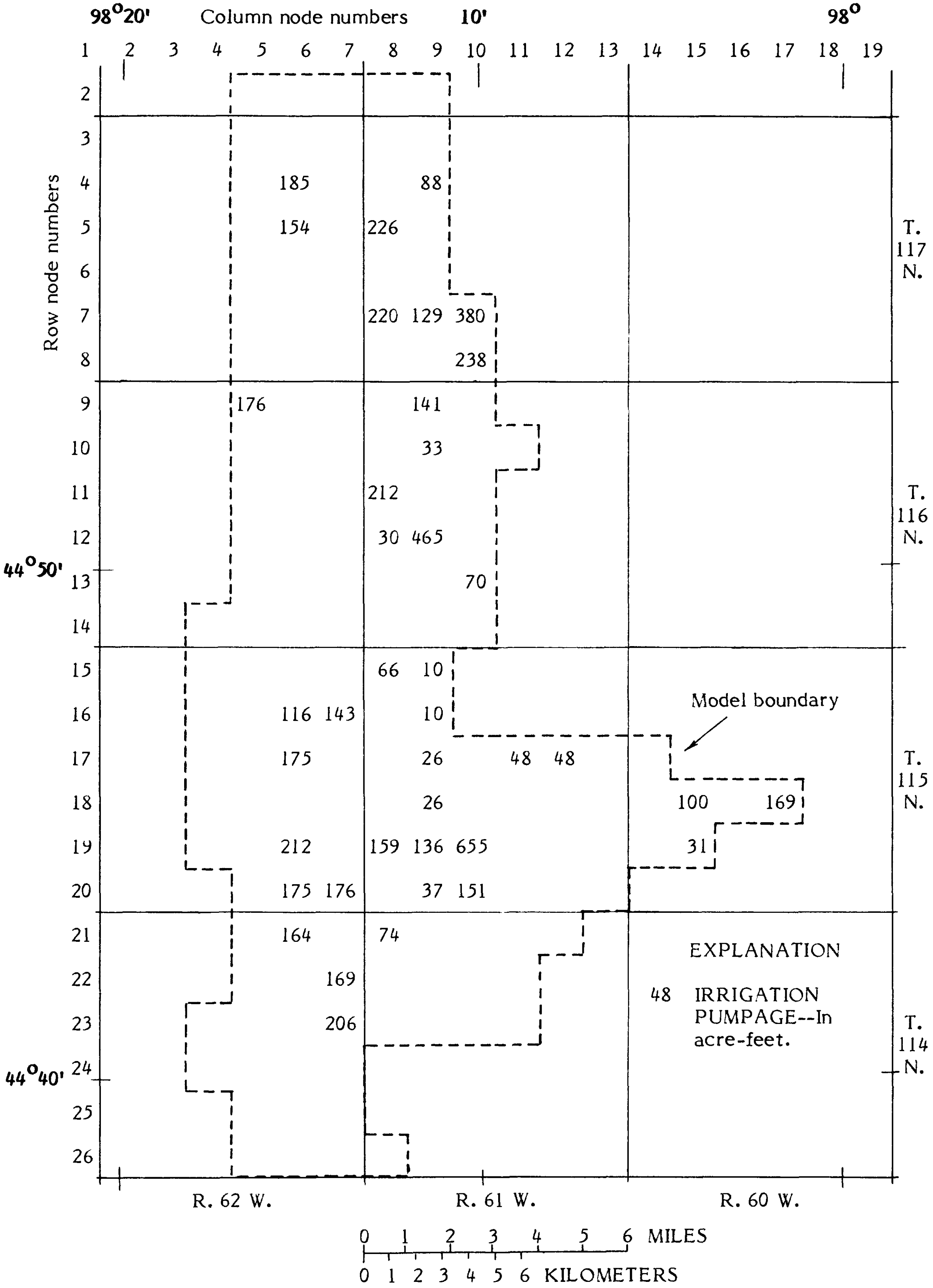

Figure 14.--Reported irrigation pumpage for 1978 in model area B.

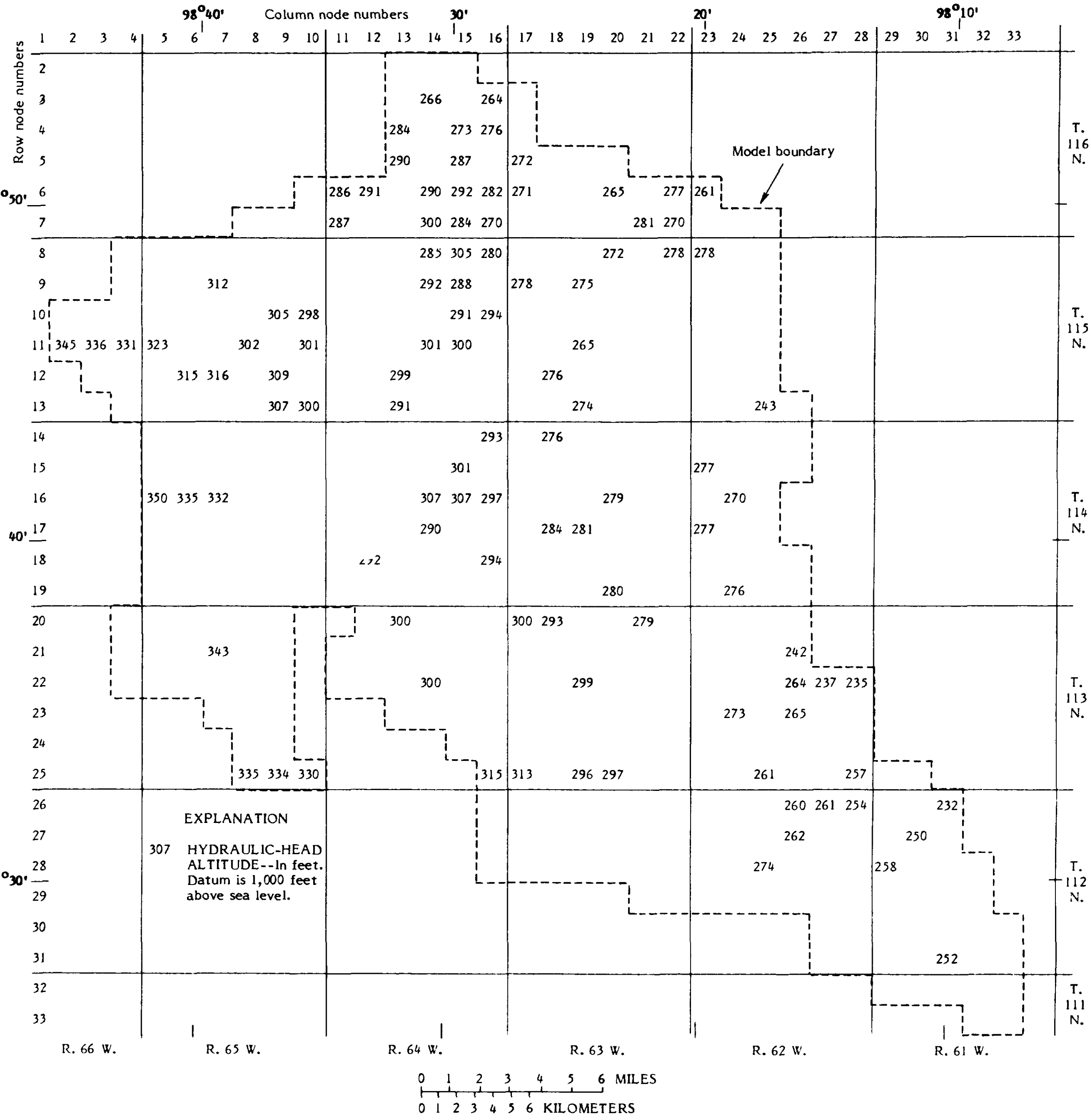

Figure 15.--Steady-state potentiometric head from observation-well data in model area A.

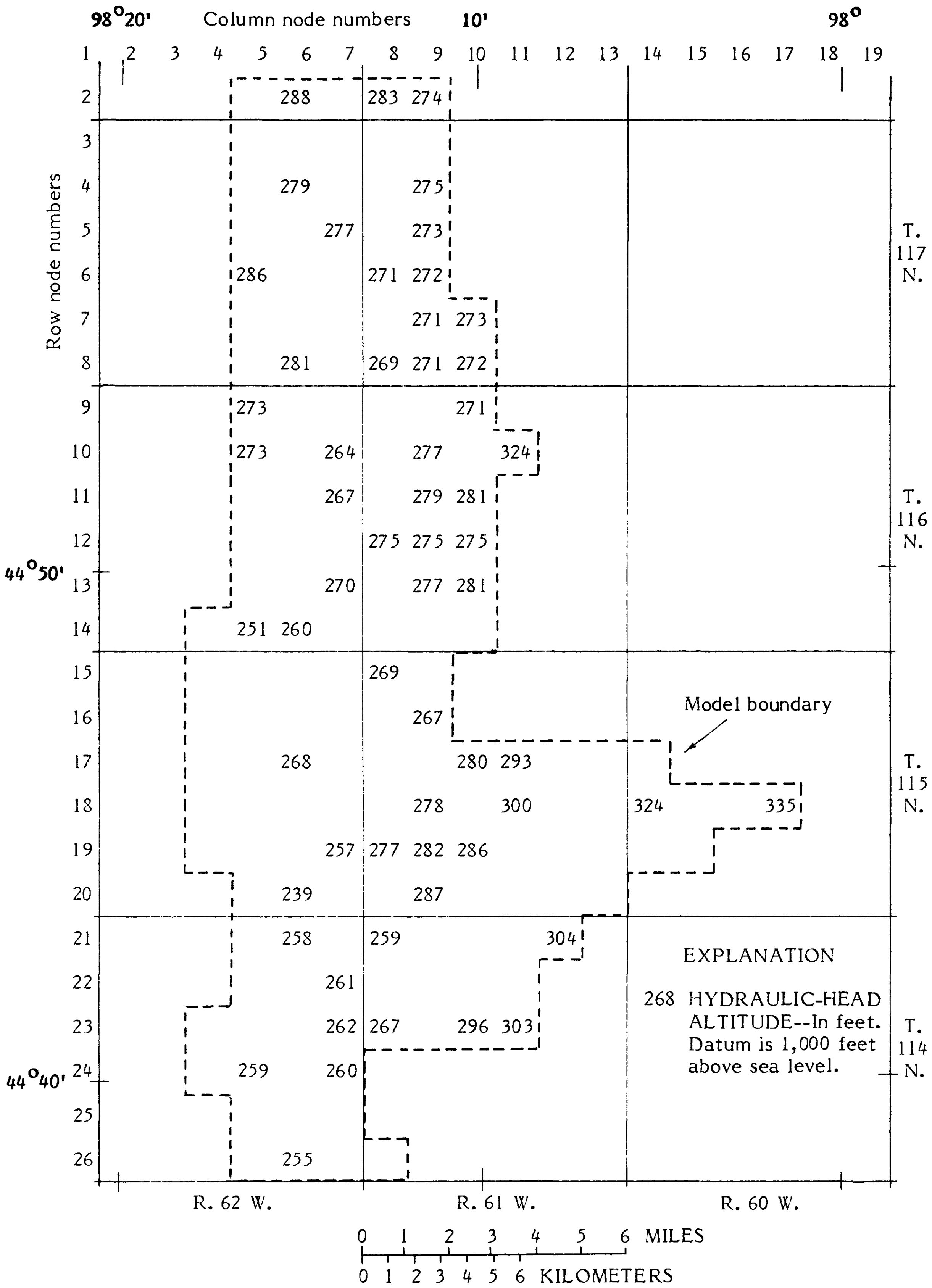

Figure 16.--Steady-state potentiometric head from observation-well data in model area B.

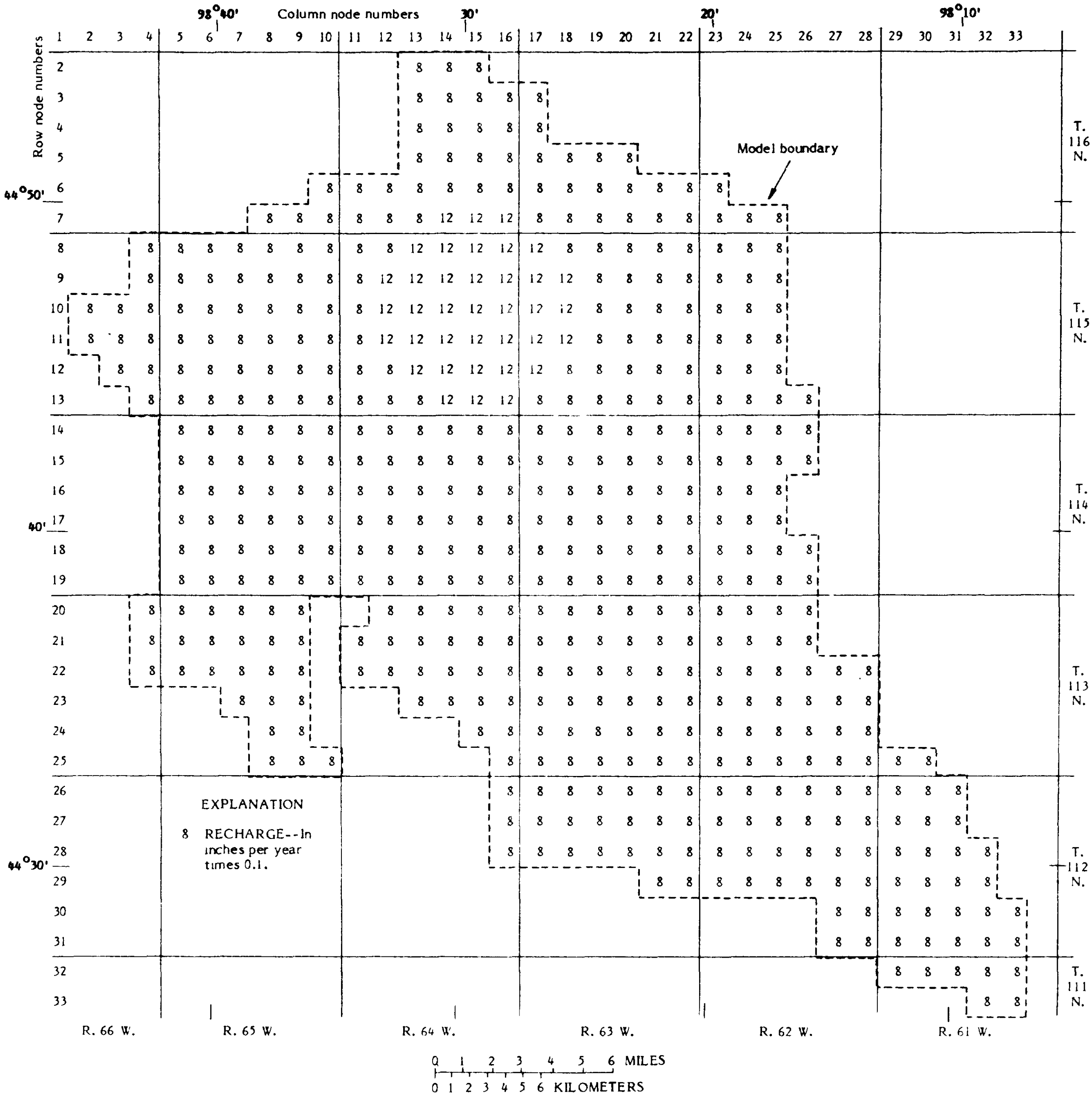

	1	2	3	4	5	6	7	8	9	10	11	12	13	14	15	16	17	18	19	20	21	22	23	24	25	26	27	28	29	30	31	32	33
2													8	8	8																		
3													8	8	8	8	8																
4													8	8	8	8	8																
5													8	8	8	8	8	8	8	8													
6										8	8	8	8	8	8	8	8	8	8	8	8	8	8										
7								8	8	8	8	8	8	12	12	12	8	8	8	8	8	8	8	8	8								
8				8	8	8	8	8	8	8	8	8	12	12	12	12	12	8	8	8	8	8	8	8	8								
9				8	8	8	8	8	8	8	8	12	12	12	12	12	12	12	8	8	8	8	8	8	8								
10		8	8	8	8	8	8	8	8	8	8	12	12	12	12	12	12	12	8	8	8	8	8	8	8								
11		8	8	8	8	8	8	8	8	8	8	12	12	12	12	12	12	12	8	8	8	8	8	8	8								
12			8	8	8	8	8	8	8	8	8	8	12	12	12	12	12	8	8	8	8	8	8	8	8								
13				8	8	8	8	8	8	8	8	8	8	12	12	12	8	8	8	8	8	8	8	8	8	8							
14					8	8	8	8	8	8	8	8	8	8	8	8	8	8	8	8	8	8	8	8	8	8							
15					8	8	8	8	8	8	8	8	8	8	8	8	8	8	8	8	8	8	8	8	8	8							
16					8	8	8	8	8	8	8	8	8	8	8	8	8	8	8	8	8	8	8	8	8								
17					8	8	8	8	8	8	8	8	8	8	8	8	8	8	8	8	8	8	8	8	8								
18					8	8	8	8	8	8	8	8	8	8	8	8	8	8	8	8	8	8	8	8	8	8							
19					8	8	8	8	8	8	8	8	8	8	8	8	8	8	8	8	8	8	8	8	8	8							
20				8	8	8	8	8	8			8	8	8	8	8	8	8	8	8	8	8	8	8	8	8							
21				8	8	8	8	8	8		8	8	8	8	8	8	8	8	8	8	8	8	8	8	8	8							
22				8	8	8	8	8	8		8	8	8	8	8	8	8	8	8	8	8	8	8	8	8	8	8	8					
23							8	8	8				8	8	8	8	8	8	8	8	8	8	8	8	8	8	8	8					
24								8	8						8	8	8	8	8	8	8	8	8	8	8	8	8	8					
25								8	8	8						8	8	8	8	8	8	8	8	8	8	8	8	8	8	8			
26																8	8	8	8	8	8	8	8	8	8	8	8	8	8	8	8		
27																8	8	8	8	8	8	8	8	8	8	8	8	8	8	8	8		
28																8	8	8	8	8	8	8	8	8	8	8	8	8	8	8	8	8	
29																					8	8	8	8	8	8	8	8	8	8	8	8	
30																											8	8	8	8	8	8	8
31																											8	8	8	8	8	8	8
32																													8	8	8	8	8
33																																8	8

Figure 17.--Estimated recharge in model area A.

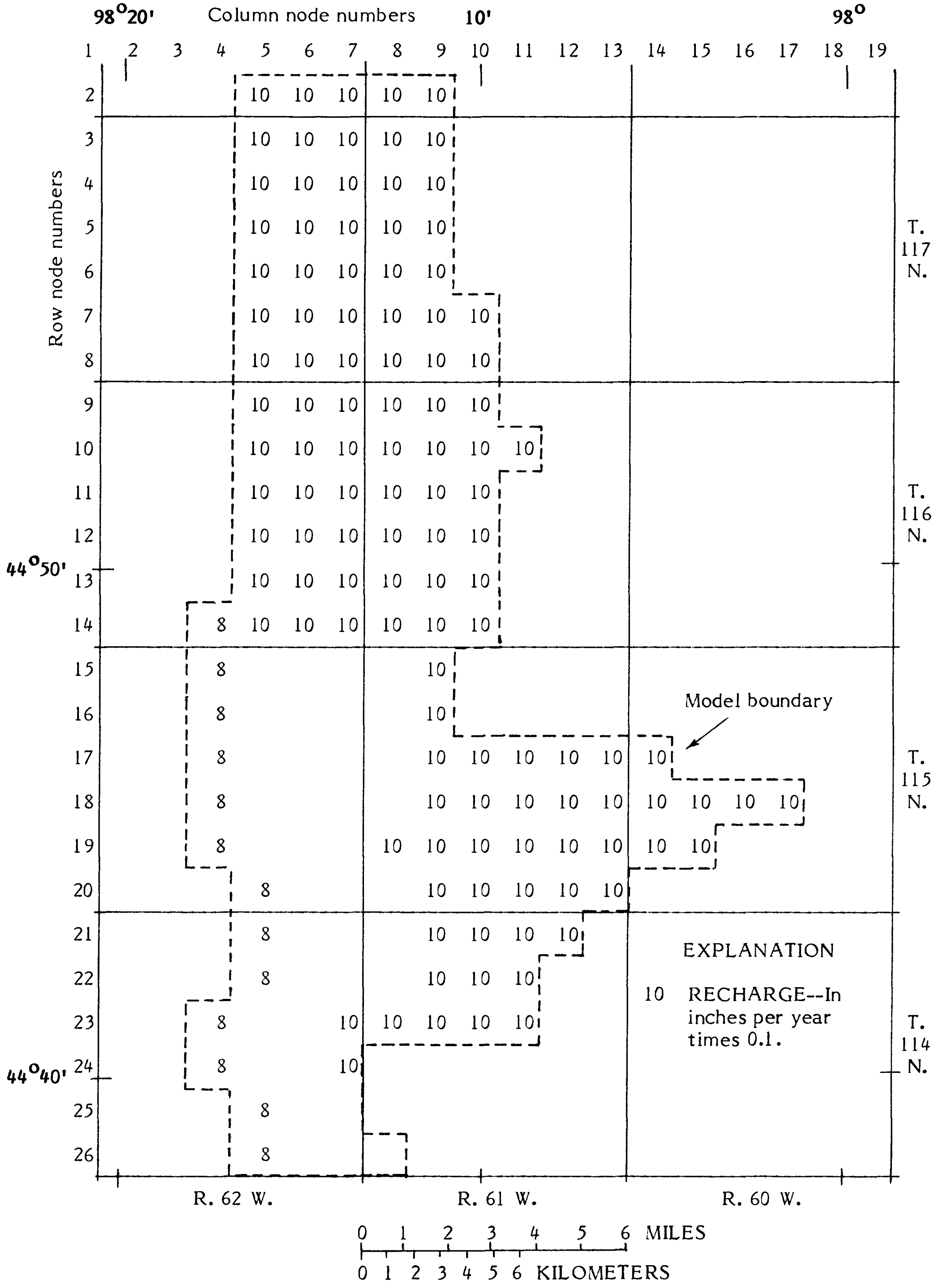

	1	2	3	4	5	6	7	8	9	10	11	12	13	14	15	16	17	18	19
2					10	10	10	10	10										
3					10	10	10	10	10										
4					10	10	10	10	10										
5					10	10	10	10	10										
6					10	10	10	10	10										
7					10	10	10	10	10	10									
8					10	10	10	10	10	10									
9					10	10	10	10	10	10									
10					10	10	10	10	10	10	10								
11					10	10	10	10	10	10									
12					10	10	10	10	10	10									
13					10	10	10	10	10	10									
14				8	10	10	10	10	10	10									
15				8					10										
16				8					10										
17				8					10	10	10	10	10	10					
18				8					10	10	10	10	10	10	10	10	10		
19				8				10	10	10	10	10	10	10	10				
20					8				10	10	10	10	10						
21					8				10	10	10	10							
22					8				10	10	10								
23				8			10	10	10	10	10								
24				8			10												
25					8														
26					8														

Figure 18.--Estimated recharge in model area B.

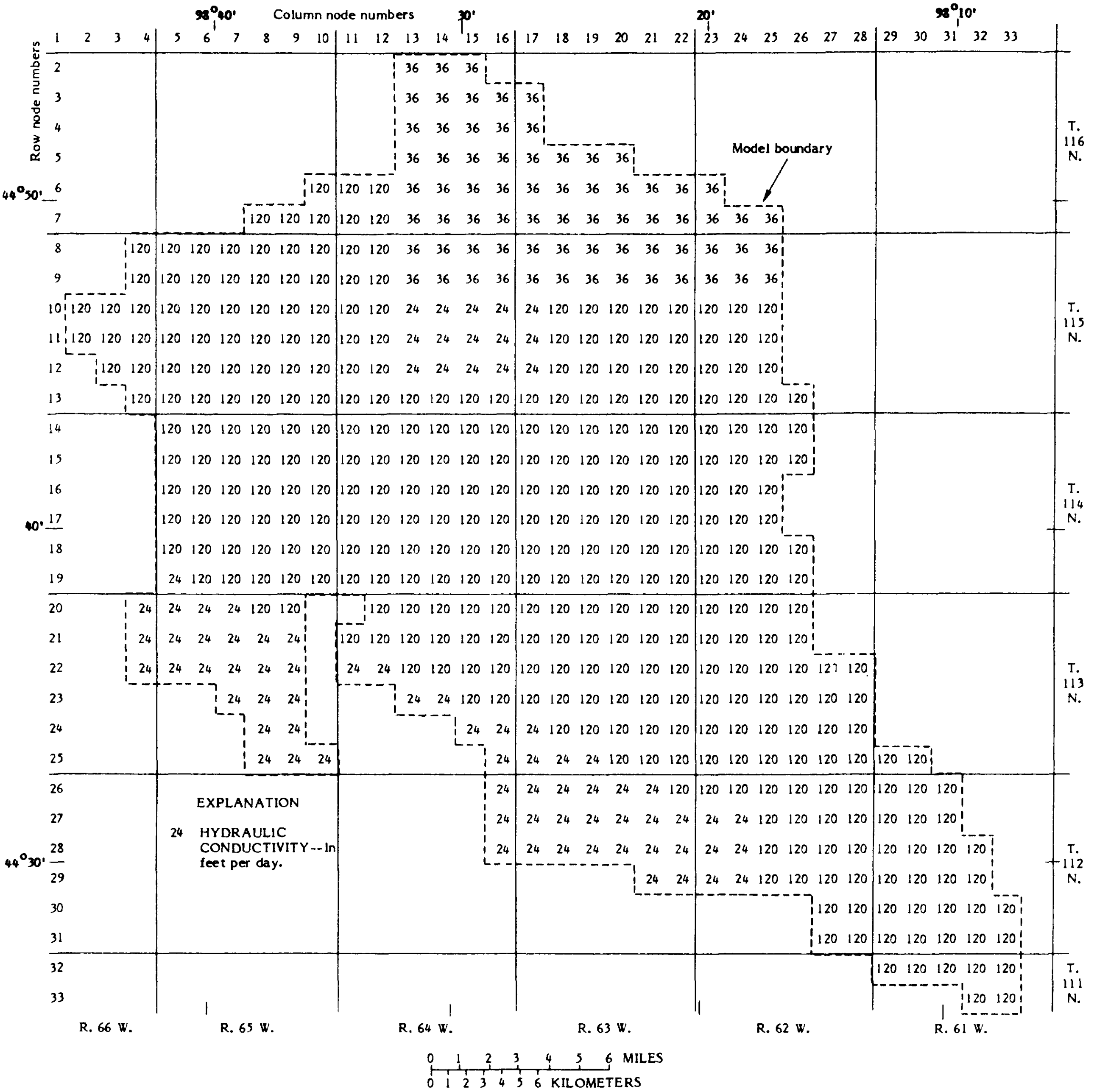

EXPLANATION

24 HYDRAULIC CONDUCTIVITY--In feet per day.

	1	2	3	4	5	6	7	8	9	10	11	12	13	14	15	16	17	18	19	20	21	22	23	24	25	26	27	28	29	30	31	32	33
2													36	36	36																		
3													36	36	36	36	36																
4													36	36	36	36	36																
5													36	36	36	36	36	36	36	36													
6										120	120	120	36	36	36	36	36	36	36	36	36	36	36										
7								120	120	120	120	120	36	36	36	36	36	36	36	36	36	36	36	36	36								
8				120	120	120	120	120	120	120	120	120	36	36	36	36	36	36	36	36	36	36	36	36	36								
9				120	120	120	120	120	120	120	120	120	36	36	36	36	36	36	36	36	36	36	36	36	36								
10		120	120	120	120	120	120	120	120	120	120	120	24	24	24	24	24	120	120	120	120	120	120	120	120								
11		120	120	120	120	120	120	120	120	120	120	120	24	24	24	24	24	120	120	120	120	120	120	120	120								
12			120	120	120	120	120	120	120	120	120	120	24	24	24	24	24	120	120	120	120	120	120	120	120								
13				120	120	120	120	120	120	120	120	120	120	120	120	120	120	120	120	120	120	120	120	120	120	120							
14					120	120	120	120	120	120	120	120	120	120	120	120	120	120	120	120	120	120	120	120	120	120							
15					120	120	120	120	120	120	120	120	120	120	120	120	120	120	120	120	120	120	120	120	120	120							
16					120	120	120	120	120	120	120	120	120	120	120	120	120	120	120	120	120	120	120	120	120								
17					120	120	120	120	120	120	120	120	120	120	120	120	120	120	120	120	120	120	120	120	120								
18					120	120	120	120	120	120	120	120	120	120	120	120	120	120	120	120	120	120	120	120	120	120							
19					24	120	120	120	120	120	120	120	120	120	120	120	120	120	120	120	120	120	120	120	120	120							
20				24	24	24	24	120	120			120	120	120	120	120	120	120	120	120	120	120	120	120	120	120							
21				24	24	24	24	24	24		120	120	120	120	120	120	120	120	120	120	120	120	120	120	120	120							
22				24	24	24	24	24	24		24	24	120	120	120	120	120	120	120	120	120	120	120	120	120	120	120	120					
23							24	24	24				24	24	120	120	120	120	120	120	120	120	120	120	120	120	120	120					
24								24	24						24	24	24	120	120	120	120	120	120	120	120	120	120	120					
25								24	24	24						24	24	24	24	120	120	120	120	120	120	120	120	120	120	120			
26																24	24	24	24	24	24	120	120	120	120	120	120	120	120	120	120		
27																24	24	24	24	24	24	24	24	24	120	120	120	120	120	120	120		
28																24	24	24	24	24	24	24	24	24	120	120	120	120	120	120	120	120	
29																					24	24	24	24	120	120	120	120	120	120	120	120	
30																											120	120	120	120	120	120	120
31																											120	120	120	120	120	120	120
32																													120	120	120	120	120
33																																120	120

Figure 19.--Estimated hydraulic conductivity in model area A.

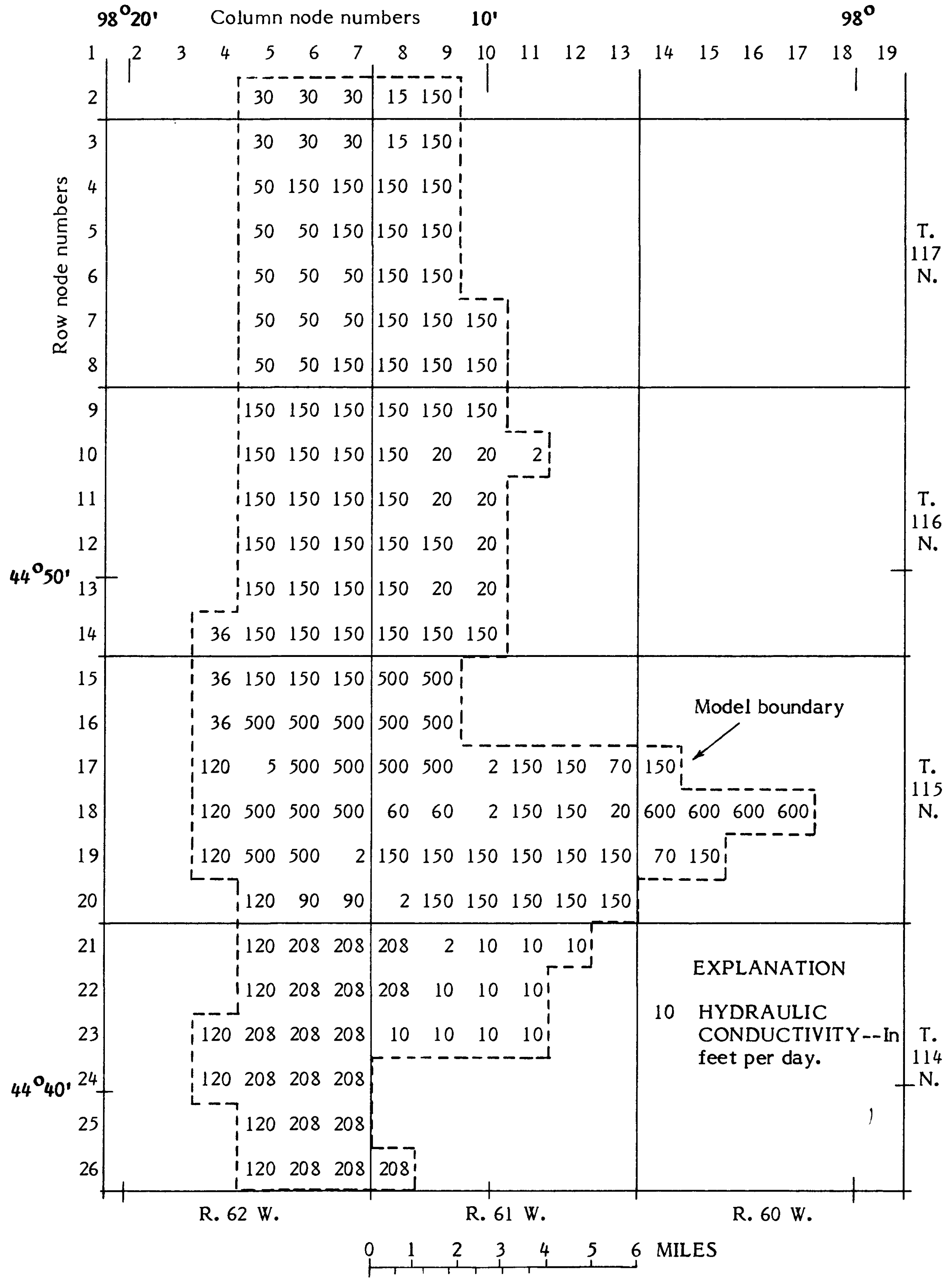

	1	2	3	4	5	6	7	8	9	10	11	12	13	14	15	16	17	18	19
2					30	30	30	15	150										
3					30	30	30	15	150										
4					50	150	150	150	150										
5					50	50	150	150	150										
6					50	50	50	150	150										
7					50	50	50	150	150	150									
8					50	50	150	150	150	150									
9					150	150	150	150	150	150									
10					150	150	150	150	20	20	2								
11					150	150	150	150	20	20									
12					150	150	150	150	150	20									
13					150	150	150	150	20	20									
14				36	150	150	150	150	150	150									
15				36	150	150	150	500	500										
16				36	500	500	500	500	500										
17				120	5	500	500	500	500	2	150	150	70	150					
18				120	500	500	500	60	60	2	150	150	20	600	600	600	600		
19				120	500	500	2	150	150	150	150	150	150	70	150				
20					120	90	90	2	150	150	150	150	150						
21					120	208	208	208	2	10	10	10							
22					120	208	208	208	10	10	10								
23				120	208	208	208	10	10	10	10								
24				120	208	208	208												
25					120	208	208												
26					120	208	208	208											

EXPLANATION

10 HYDRAULIC CONDUCTIVITY--In feet per day.

Figure 20.--Estimated hydraulic conductivity in model area B.

Figures 21-27 show results for a steady-state model solution with $I = 0$. Figure 21 shows a contoured surface for hydraulic head made from the h_i as produced by the model. Figures 22 and 23 show the discrepancy between these h_i and the $\hat{h}_i$ of figures 15 and 16. Figures 22 and 23 are figures 15 and 16 subtracted from the h_i represented by figure 21. The average discrepancy between h_i and h_i was 0.21 ft and 0.88 ft for model areas A and B respectively. S_{err} of equation (5) was 5.28 ft and 3.52 ft for model areas A and B respectively. Figures 24 and 25 show $(D + E_2)_i$ in units of 10^3 ft^3/d (0.16 in/yr over the area of a node). Note that the maximum value of $(D + E_2)_i$ is 95,000 ft^3/d or 15 in/yr over the area of a node, a value much smaller than the open-pan evaporation rate of 49 in/yr. Figures 26 and 27 show a blank for a confined condition in the aquifer at node i and a 0 when a water-table condition exists. For model area A: I, R, F, and $(D + E_2)$ of (1) had the values 0, 2,768, -271, and 3,037, respectively, again in units of 10^3 ft^3/d, or 0, 0.829, -0.081, and 0.905 in/yr over the 527 mi^2 of area A. For model area B: I, R, F, and $(D + E_2)$ had the values 0, 811, 23, and 789 in units of 10^3 ft^3/d, or 0, 0.762, 0.022, and 0.742 in/yr over the 167 mi^2 of area B. Because the numerical solution of the model is approximate, these values do not satisfy equation (1) exactly. The values for R are the sum of the values for R_i shown in figures 17 and 18 with an appropriate change of units.

As mentioned above, figures 24 and 25 show $(D + E_2)_i$. Except for the nodes along the James River, the discharges to streamflow $(D)_i$ are equal to zero, so that for these nodes the values shown are the evapotranspiration $(E_2)_i$ by itself. Summing the discharges $(D + E_2)_i$ for the nodes along the James River from figures 24 and 25 gives a value of 1,610 ft^3/d, which is approximately 9.6 percent of the average flow of the river upstream 6 mi from the aquifer at Redfield, and approximately 7.8 of the average flow of the river downstream 4 mi from the aquifer at Huron. Stream-gage measurements at Redfield and Huron show no apparent gain in stream base flow between the two stations. However, the measurements are not accurate enough to eliminate the possibility that all of the 1,610 ft^3/d could be discharge to streamflow D. Thus, the share of the discharges $(D + E_2)_i$, in figures 24 and 25, taken up by $(D)_i$ and $(E_2)_i$ separately is unknown for the nodes along the river.

Crop production in the river nodes tends to be better than in those nodes with $(E_2)_i = 0$, suggesting that the evapotranspiration rates $(E_2)_i$ into the river nodes are large enough to make a noticeable difference in crop yield. This observation would suggest that the evapotranspiration rates $(E_2)_i$ might be a substantial fraction of the discharges $(D + E_2)_i$.

Time-dependent calibration, with R_i and I_i functions of time, was done by matching $h_i(t)$ with $\hat{h}_i(t)$. The hydraulic heads $h_i(t)$ were determined by the model at times $t = t_n$ separated by time intervals Δt equal to 365 days or (365/12) days.

For $\Delta t = 365$ days, figures 28-33 show hydrographs for six observation wells and also aquifer model-calculated values for $h_i(t_n)$. Times t_n, $n = 1,11$, occur at the end of the years 1968-78, an eleven-year period of nearly average rainfall and assumed average recharge. The best overall fit of $h_i(t_n)$ and $\hat{h}(t_n)$ for a total of 14 observation wells was obtained when the $(R_i)_n$, $n = 1,11$ for the years 1968-78, had the values of those in figures 17 and 18 for steady-state calibration multiplied by the factors of 1.0, 1.2, 1.0, 1.7, 2.1, 1.2, 0.0, 0.0, 0.0, 1.4, and 1.4. Note that the sum of these 11 factors totals 11.0, so that their average value is 1.0. It was assumed that the spatial variation of $R_i(t)$ was the same each year and as given by figures 17 and 18. The factors above can be approximated by assuming that a certain fraction α of the excess of precipitation over 18 in for a given year is recharged that same year, and an equal amount the next year. The fraction α, the same for each year, is found by normalization.

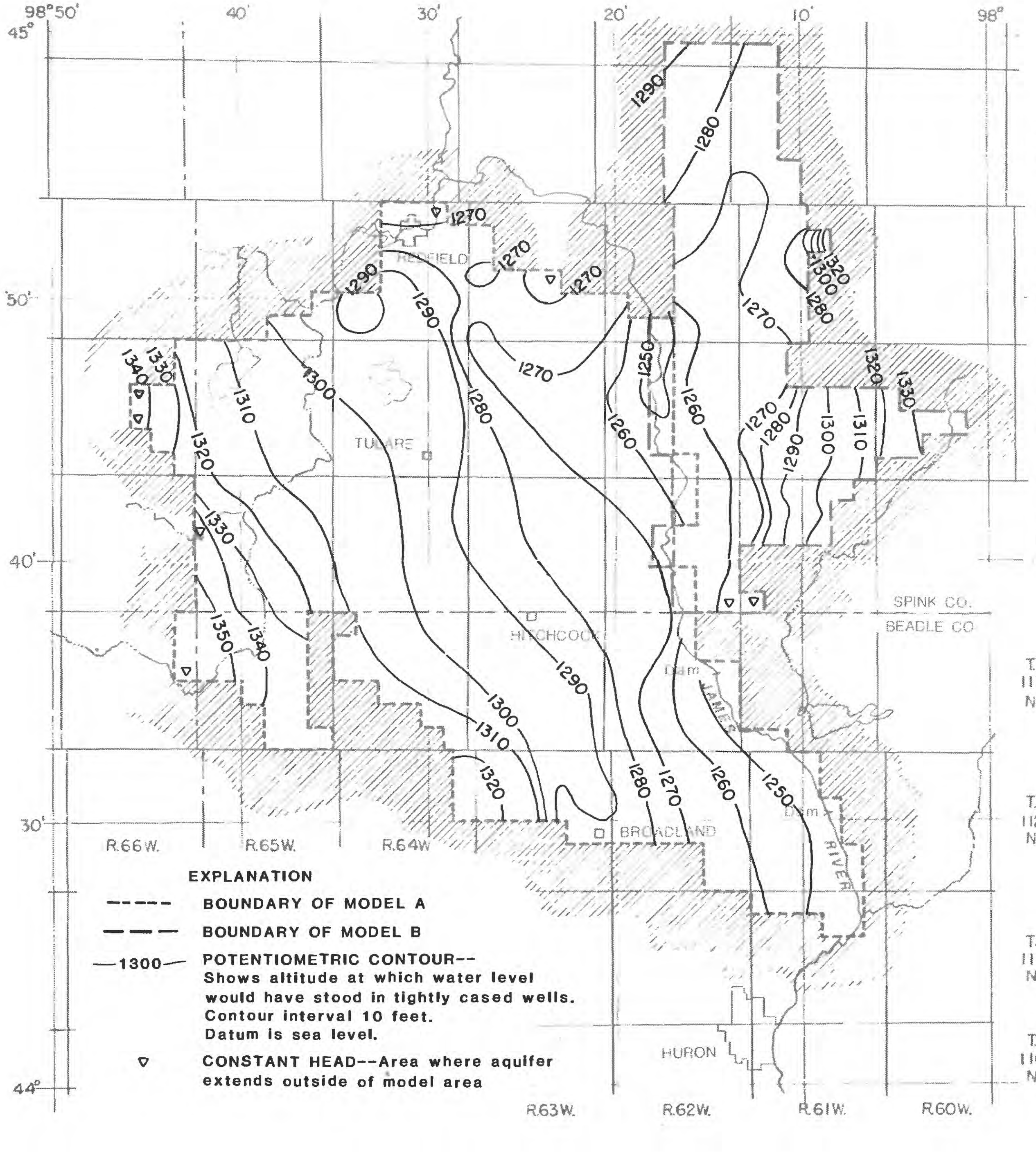

Figure 21.--Hydraulic head from a steady-state aquifer model solution with no irrigation.

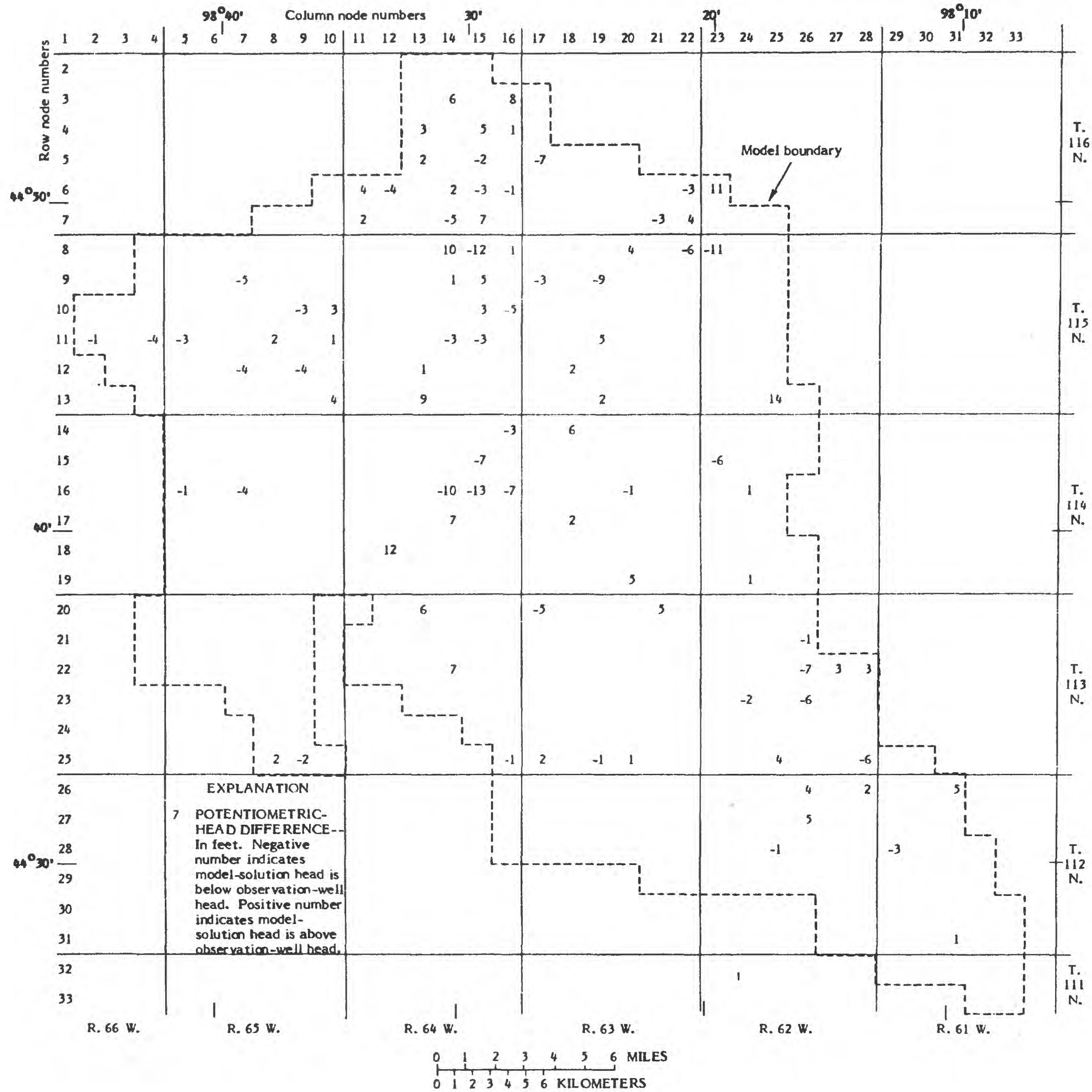

Figure 22.--Difference between steady-state head from observation-well data and head from model solution with no irrigation in model area A.

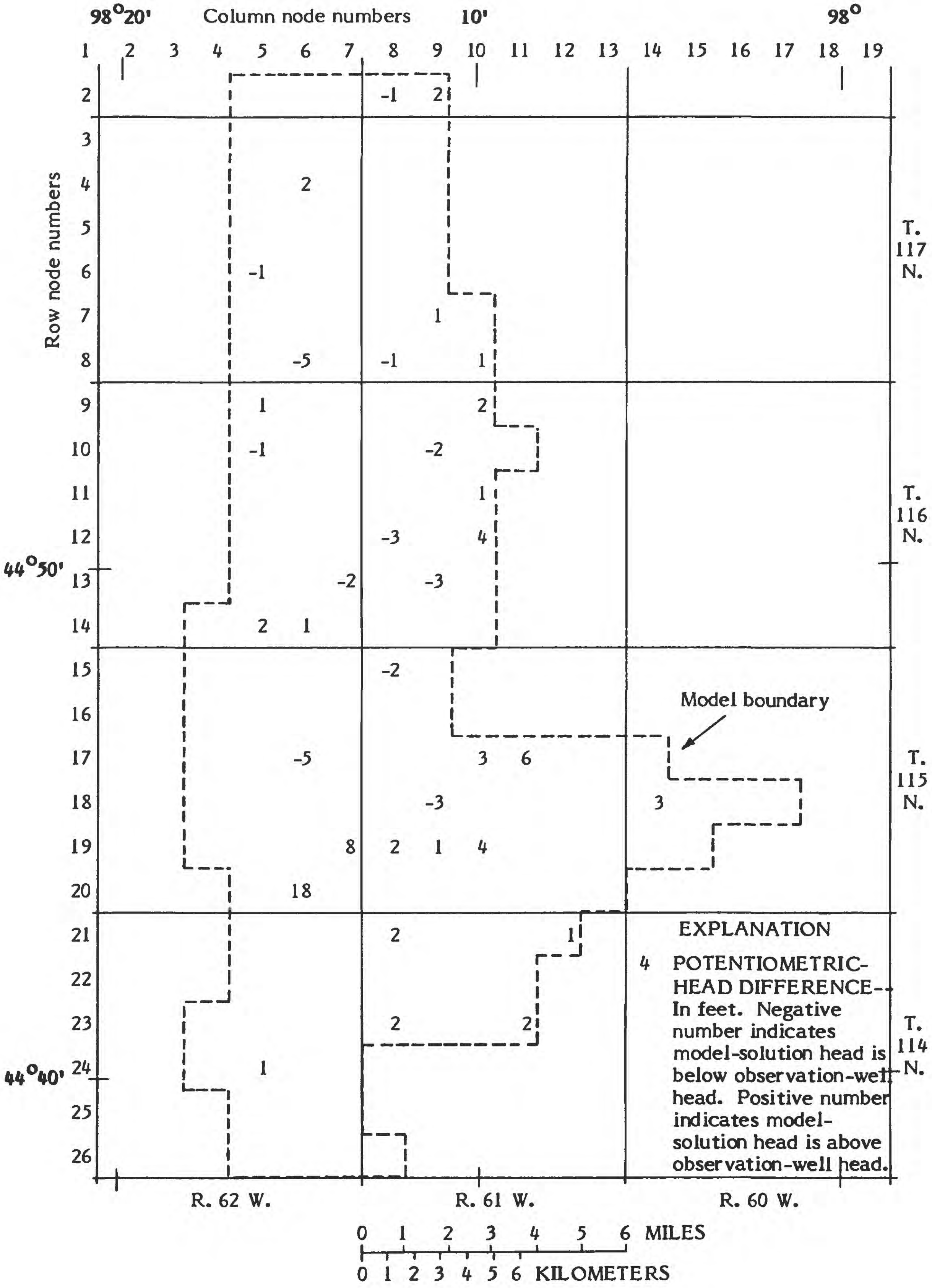

Figure 23.--Difference between steady-state head from observation-well data and head from model solution with no irrigation in model area B.

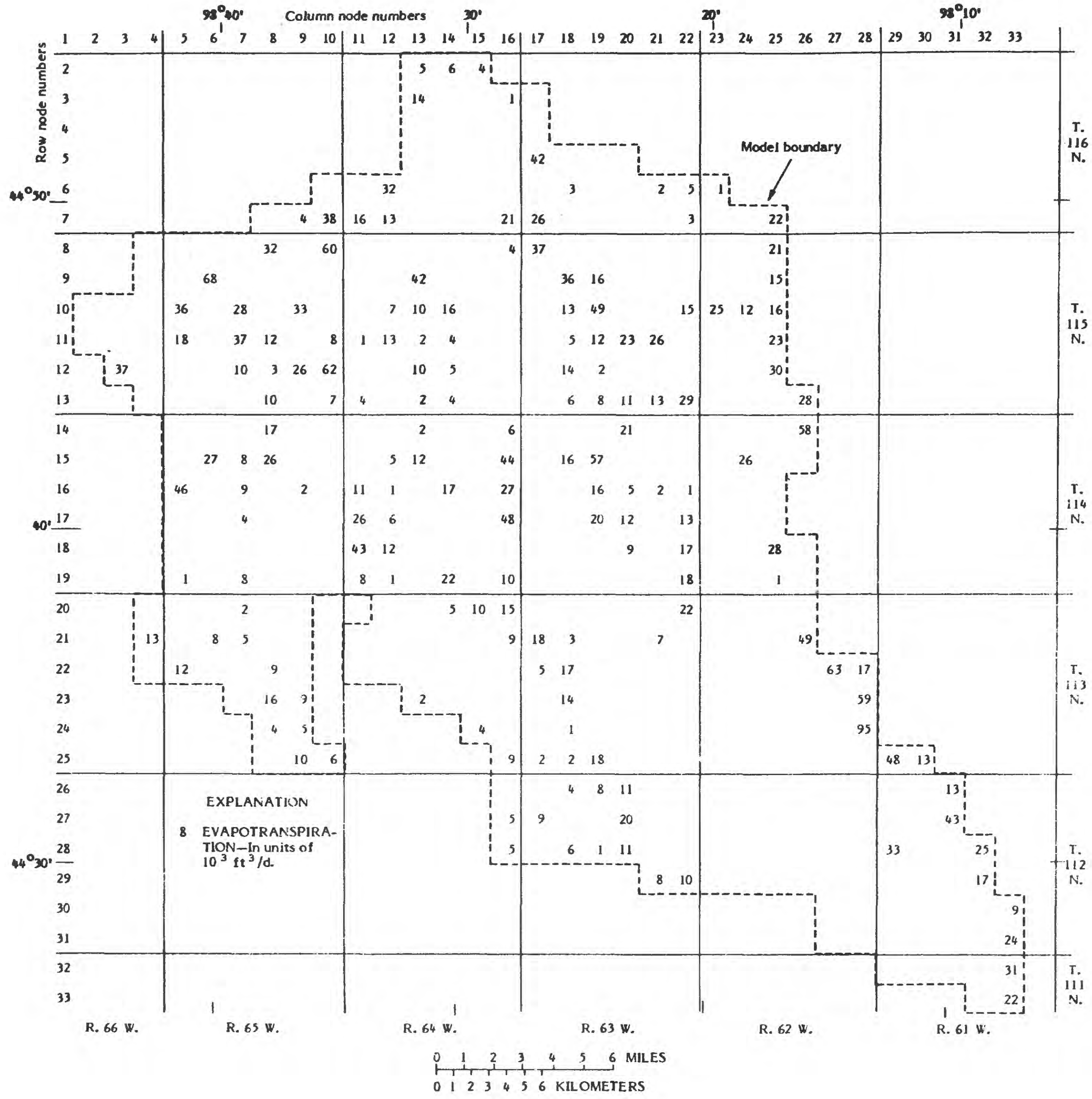

Figure 24.--Evapotranspiration from a steady-state model solution in model area A.

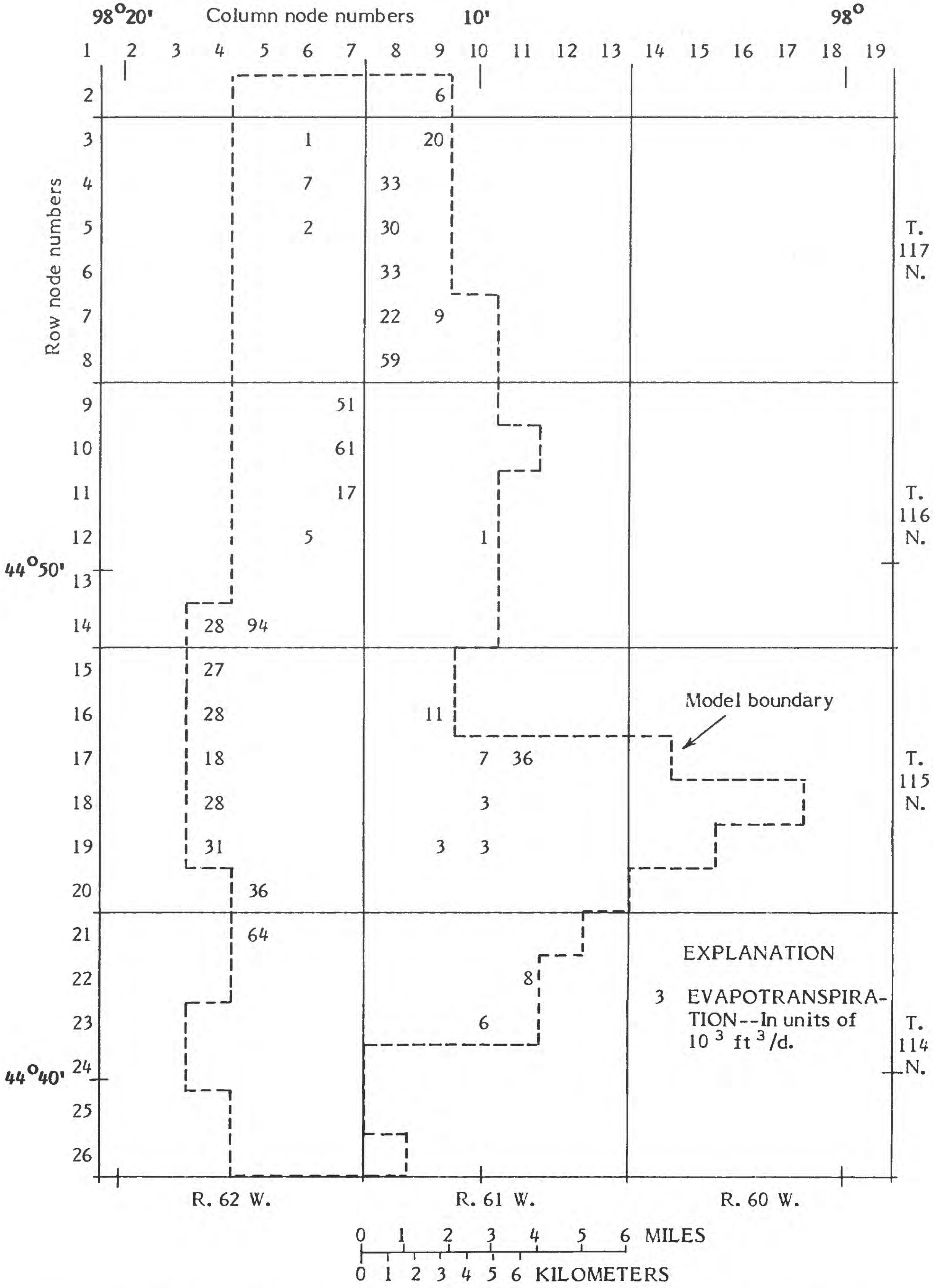

Figure 25.--Evapotranspiration from a steady-state model solution in model area B.

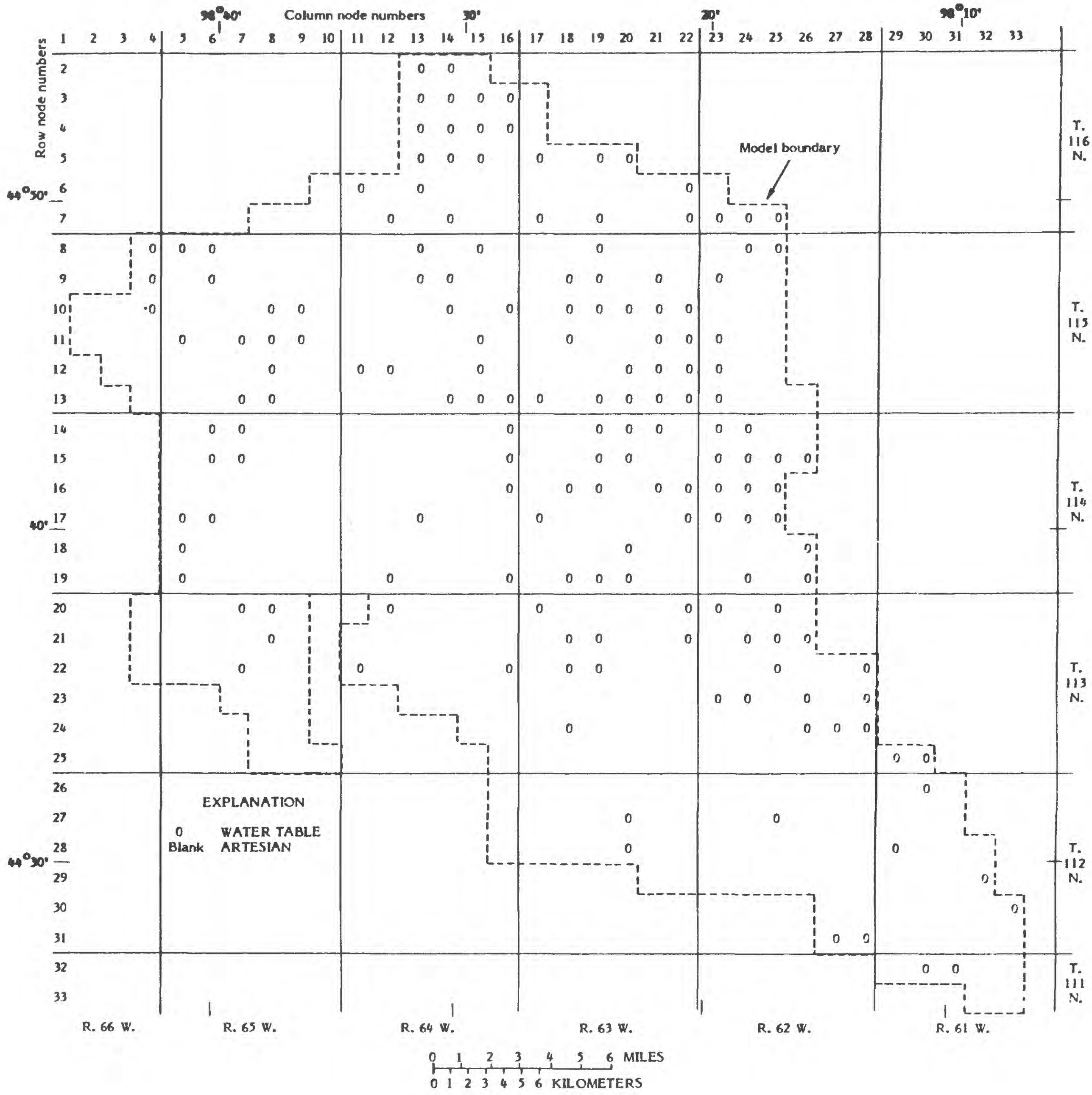

Figure 26.--Location of water table and artesian areas for the steady-state model soltuion in model area A.

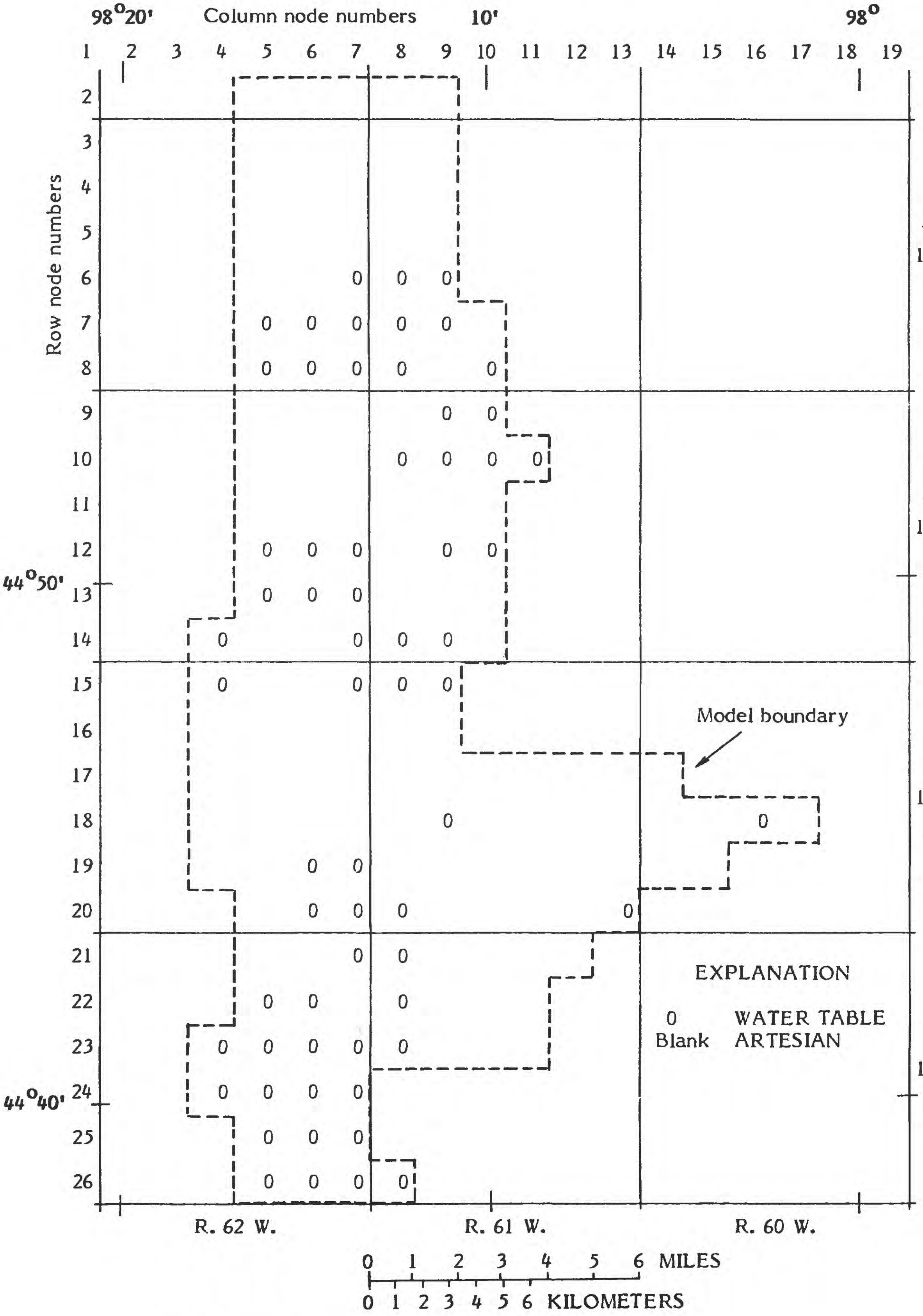

Figure 27.--Location of water table and artesian areas for the steady-state solution in model area B.

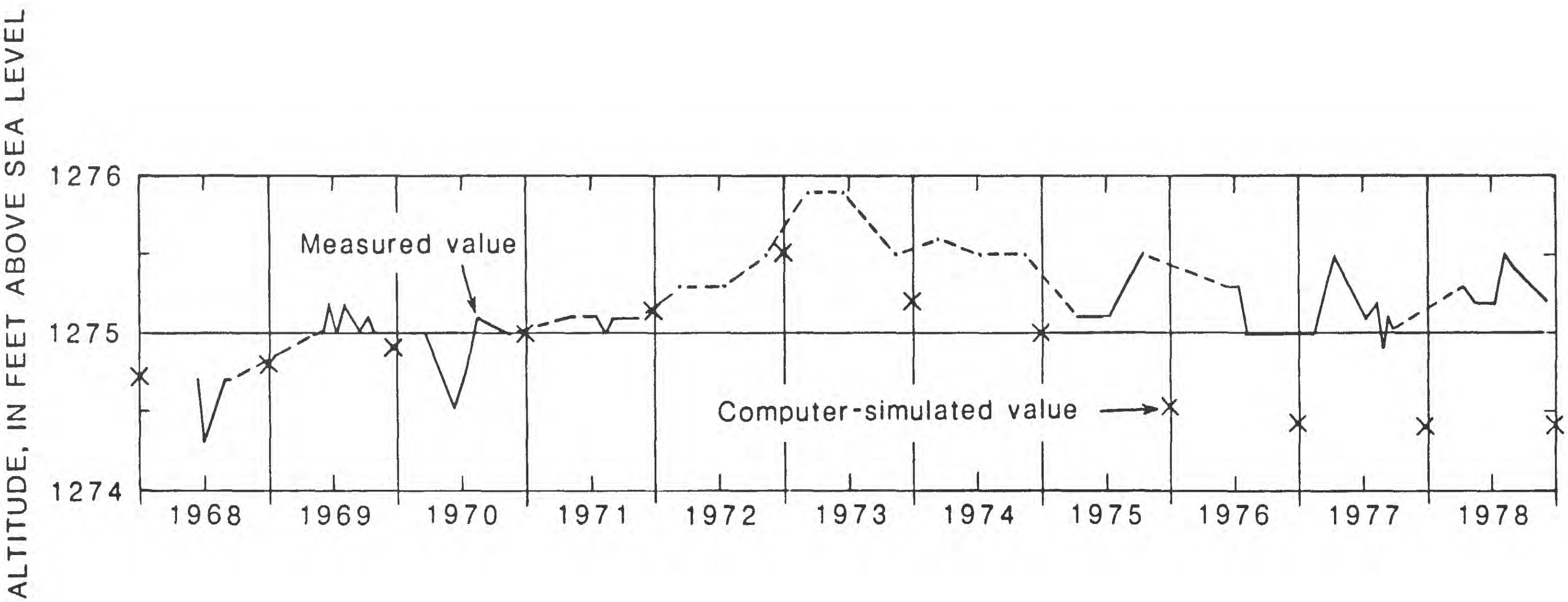

Figure 28.--Hydrograph for well 115N63W33DDC and year-end model-calculated hydraulic head values.

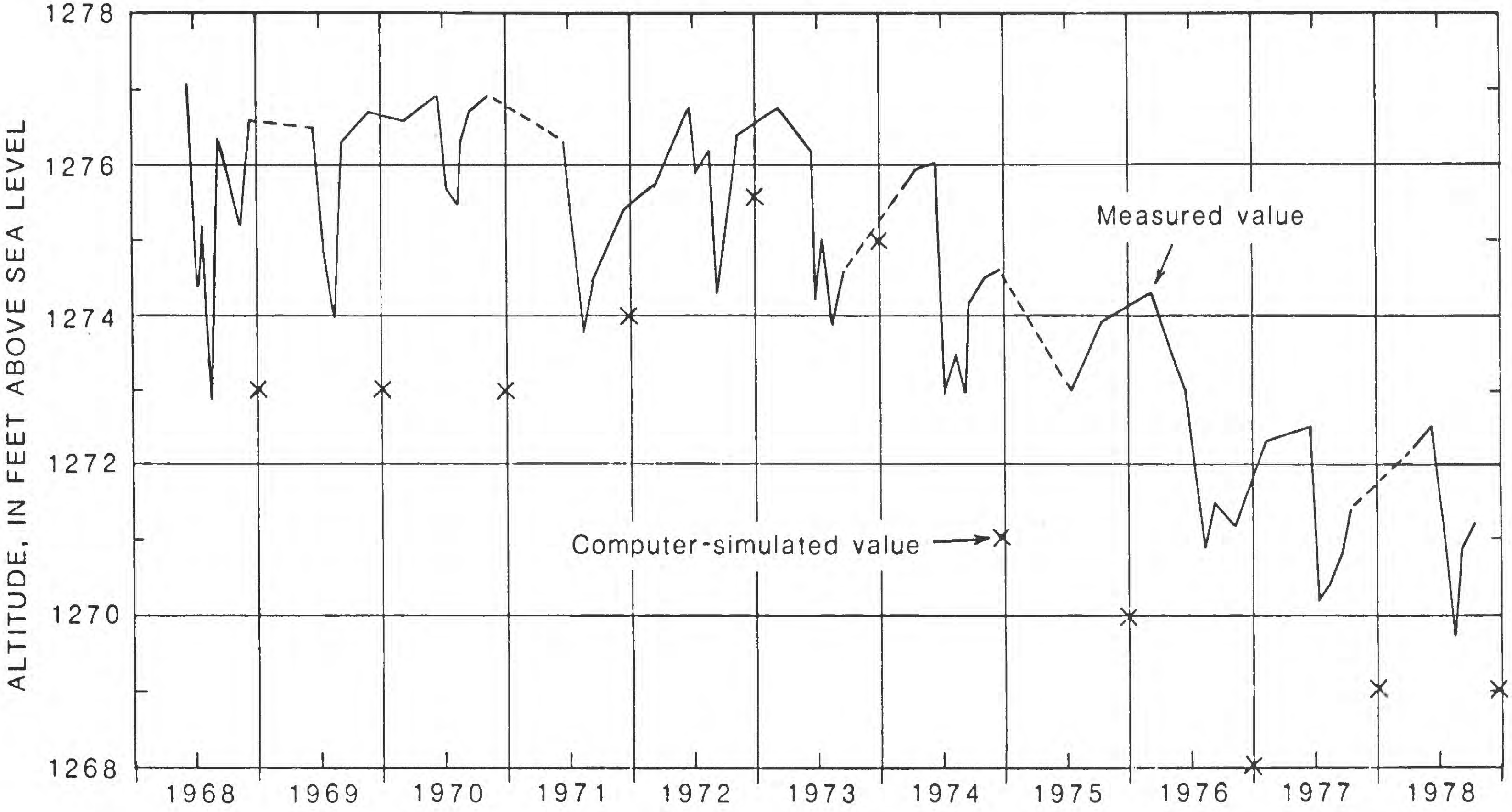

Figure 29.--Hydrograph for well 116N61W29DDAA and year-end aquifer model-calculated hydraulic head values.

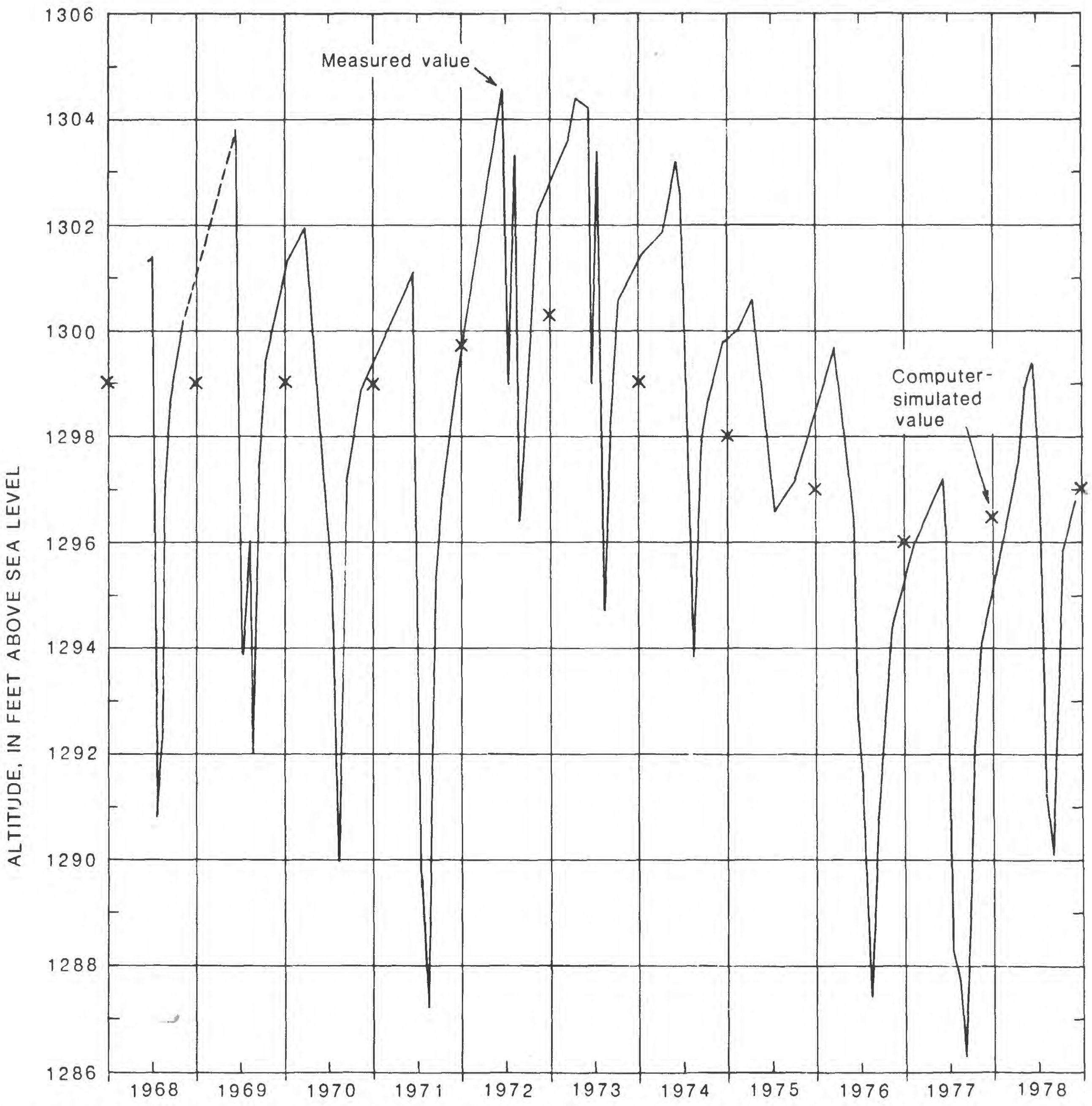

Figure 30.--Hydrograph for well 115N64W28BBBB and year-end aquifer model-calculated hydraulic head values.

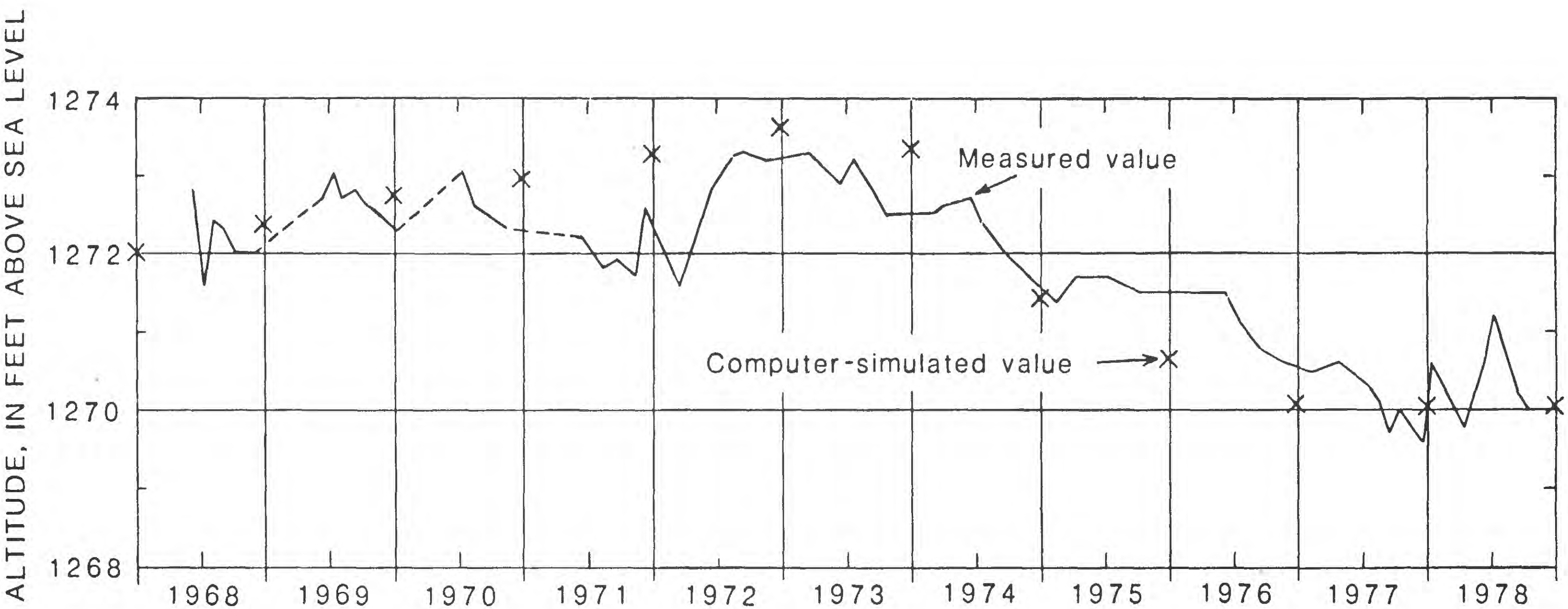

Figure 31.--Hydrograph for well 117N61W16CCCC and year-end aquifer model-calculated hydraulic head values.

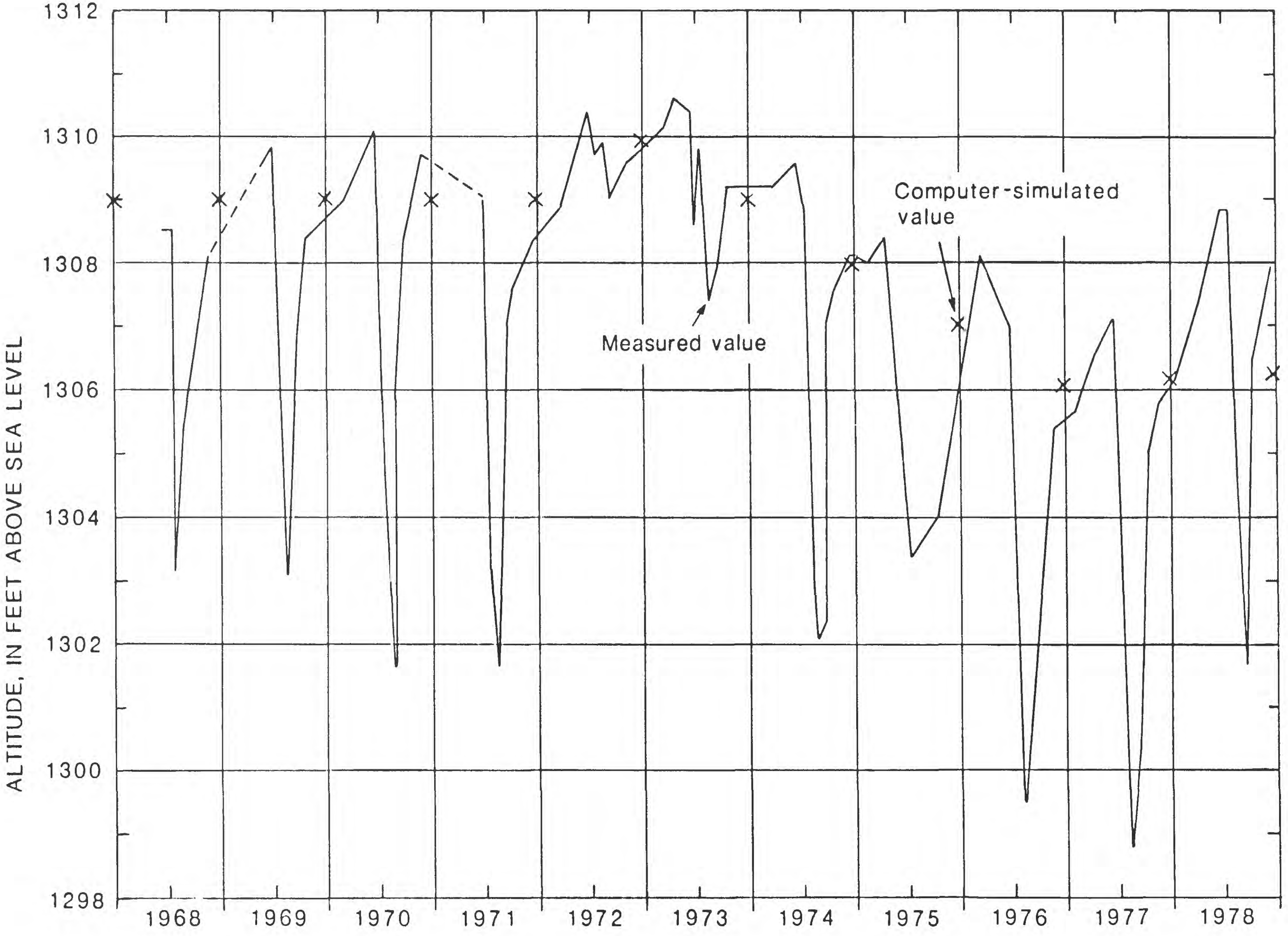

Figure 32.--Hydrograph for well 115N65W35ABB and year-end aquifer model-calculated hydraulic head values.

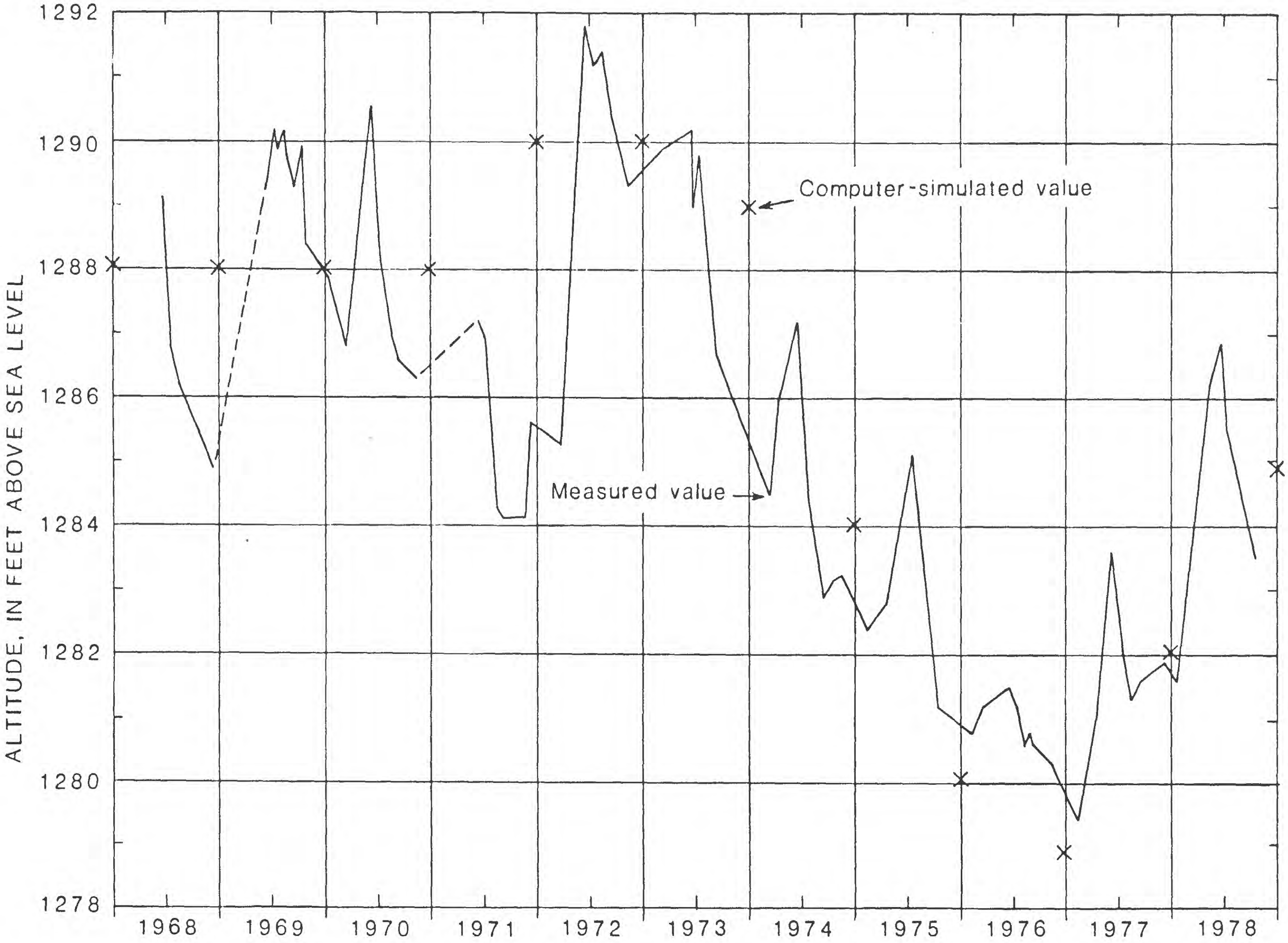

Figure 33.--Hydrograph for well 118N62W35B and year-end model-calculated hydraulic head values.

The I_i as functions of time were determined from reported irrigation groundwater use data. Use in the entire James River basin for the years of 1973-78 was 11,490, 10,858, 13,449, 38,238, 45,168, and approximately 48,000 acre-ft respectively. Dividing these values by the 1978 value and multiplying by 1.2 gives: 0.29, 0.27, 0.37, 0.96, 1.13, and 1.2. The I_i used for the years 1968-78 in the calibration were the I_i of figures 13 and 14 multiplied by 0.0 for the years 1968-72 and the above factors for the years 1973-78. Thus the spatial variation of the I_i was assumed to be the same each year and to be that of the year 1978, an approximation to actual irrigation water use. The factor 1.2 was inserted to compensate for the fact that approximately 70-85% of the irrigators responded to the irrigation water-use questionnaire which was sent to each of them each year. For model area A and the year 1978: I, R, F, $(D + E_2)$, and $\Delta S/\Delta t$, of (4) had the values 1,170, 3,875, -274, 2,473, and 506 10^3 ft^3/d respectively. For area B, these values were 863, 1,135, 20, 546, and -294 10^3 ft^3/d respectively. For area A, the aquifer model gave an average decline in the hydraulic head of 1.1 ft for the 11-year period 1968-78. For area B, the decline was 3.2 ft. The previously described $I = 0$ steady-state solution was assumed for the initial condition of the aquifer at the beginning of the year 1968. Over the period 1968-78, note that $(D + E_2)$ changed from 3,037 to 2,473 and from 789 to 546 10^3 ft^3/d for model areas A and B.

Time-dependent calibration was also done with $\Delta t = (365/12)$ days. In this case $t_n = [(365/12) \text{ days}]\, n$, $n = 1,12$. The $h_i(t_n)$ produced by the aquifer model were compared with $\hat{h}_i(t_n)$ from observation-well hydrographs. The hydrographs in figures 28-33 show that the hydraulic head can have considerable variation in a 365-day period. The hydrographs for figures 29, 30, and 32 show a sharp low in the months of July or August, probably due to the proximity of one or more irrigation wells. In all of the hydrographs, recharge usually causes the hydraulic head to rise each year between fall and late spring or early summer. In order for the model to reproduce each hydrograph, it would be necessary to meticulously adjust the parameters: $R_i(t_n)$, b_i, the n dependence of the rate of increase of $(D + E_2)_i$ with h_i, k_i, $(S_y)_i$, and S_i, for all i. It would also be necessary to be sure than $I_i(t_n)$ was correct for each i and n. Such meticulous and detailed i dependent calibration was not attempted because it does not significantly increase the ability of the model to make long-term predictions.

The i dependence of the $R_i(t_n)$ was assumed to be that of figures 18 and 19. The $R_i(t_n)$ were set equal to the R_i of those figures multiplied by 0.0, 0.0, 2.0, 5.0, 4.0, 1.0, 0.0, 0.0, 0.0, 0.0, 0.0, and 0.0 for $n = 1,12$ corresponding roughly to the months of January through December. This n dependence of $R_i(t_n)$ places all recharge in the 4 months of March, April, May, and June, and gave the best fit between observed and model produced heads. The n dependence of the rate of increase of $(E_2)_i$ with h_i was set proportional to the monthly pan-evaporation rate. For $n = 1,12$, the rate of increase of $(E_2)_i$ with h_i was given by 0.0, 0.0, 0.0, 1.3, 1.7, 2.1, 2.4, 2.0, 1.5, 1.0, 0.0, and 0.0 multiplied by the value used for steady-state calibration. These values are those from steady-state calibration. The $I_i(t_n)$ were set equal to the I_i of figures 13 and 14 multiplied by 0.0, 0.0, 0.0, 0.0, 0.0, 2.0, 3.0, 4.0, 3.0, 0.0, 0.0, and 0.0, for $n = 1,12$. This prescription for the $I_i(t_n)$ is approximated from monthly irrigation data and places all irrigation in the 4 months of June through September. With the above prescriptions for $R_i(t_n)$, the rate of increase of $(E_2)_i$ with h_i, and $I_i(t_n)$, the agreement between $\hat{h}_i(t_n)$ and $h_i(t_n)$ was in some cases rather poor. From observation-well hydrographs for the years of 1977 and 1978, the maximum yearly variation of the hydraulic head h, for each of 25 observation wells, was tabulated. The average of these 50 values was 3.0 ft. The average of these values as determined by the model, with $\Delta t = (365/12)$ days, was 2.9 ft. Thus, although individual hydrographs could not usually be matched by the model, their average behavior was duplicated quite well.

The stated purpose of this study is to predict the ability of the aquifer to supply water for irrigation in the future. Steady-state solutions were found or attempted using the I_i from figures 13 and 14 multiplied by 1.2. As explained previously, this rate should be approximately equal to the actual use rate for the year 1978. The R_i were taken from figures 17 and 18 and are recharge rates for an average year. For aquifer area A, equation (1) was:

$$1{,}170 = 2{,}768 - (-292) - 1{,}880$$

$$0.349 = 0.829 - (-0.087) - 0.560$$

$$I = R - (F) - (D + E_2).$$

The first equation has the units of 10^3 ft^3/d, the second in/yr over the 527-mi^2 area of model area A. Note that R is substantially larger than I. If we suppose this recharge R above is correct, then it follows that area A could sustain substantially greater irrigation water pumpage, perhaps even twice as much if wells were located properly. Area A of figure 34 shows a contoured surface made from the h_i as produced by the model. The average decline in the hydraulic head below that of the steady-state $I = 0$ solution was 2.9 ft. Despite the decline in the hydraulic head, the James River flood plain still serves as the major sink for ground-water flow.

The situation with model area B is quite different. The sum of the R_i from figure 18 is 811×10^3 ft^3/d or 0.762 in/yr over the 167-mi^2 area of model area B. The sum of the I_i from figure 14 multiplied by 1.2 is 863×10^3 ft^3/d which is greater than recharge R. Clearly, since E_2 cannot be negative unless (D + F) is negative and large enough to make up the difference between I and R, there can be no steady-state solution. An attempted steady-state solution failed. A solution could not be found because the irrigation pumpage was not able to reverse or stop the flow to the nodes along the James River and F also remained positive, even though drawdown was enough to produce many dry nodes. It follows that the model predicts that model area B will not be able to continue irrigation at 1978 use rates for an indefinite period. A time-dependent model simulation with the I_i constant and equal to 1.2 times those of figure 14, and the R_i constant and from figure 18 was carried out for an elapsed time of 50 years beginning with the steady-state $I = 0$ solution. At the end of this period, 6 nodes had gone dry. The average decline in hydraulic head during the 50-year period was 13.5 ft. Area B of figure 34 shows a contoured surface made from the h_i as produced by the model at the end of the 50-year period. The nodes which went dry are denoted by the symbol d. The model thus predicts that although 1978 use rates cannot be continued indefinitely, they should be able to continue, for the most part, for a period of perhaps 50 years. Some decrease in well yield is to be expected during this period however.

OTHER PREDICTIVE TOOLS

Equation (4), $I = R - (F) - (D + E_2) - \Delta S/\Delta t$, expresses the conservation of water in the aquifer. Inflow to the aquifer occurs from recharge R. Evapotranspiration E_2 removes water from the aquifer. Water provided by recharge R is a source of water for irrigation I. F can be negative and also provide water for irrigation I. In this study, recharge R is approximately independent of I and the hydraulic head h in the aquifer. However, $(D + E_2 + F)$, the rate of loss of water from the aquifer, increases as h rises. This situation is like that of a barrel with a V shaped wedge cut in its side and opening

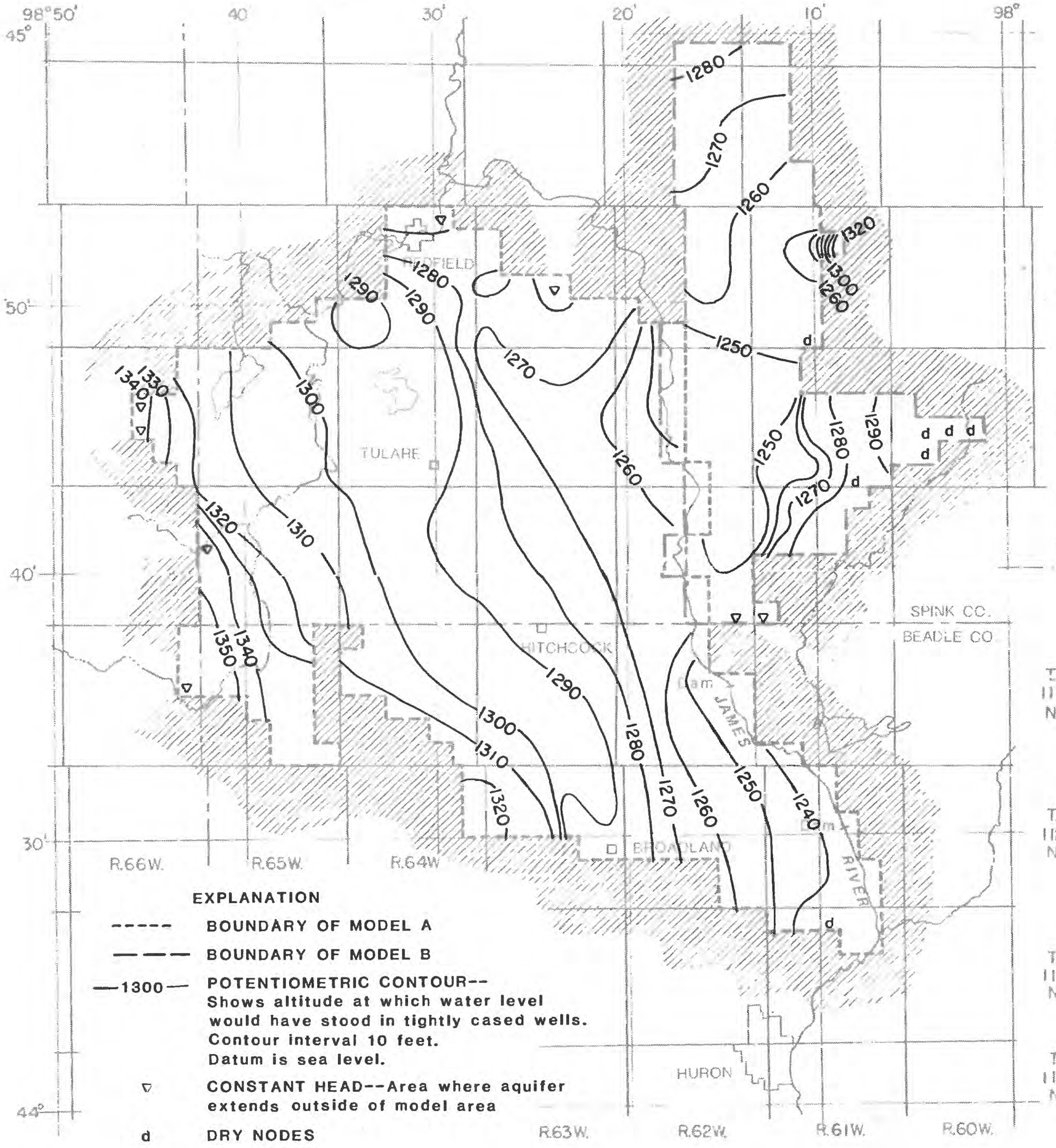

Figure 34.--Hydraulic head from aquifer model solutions with irrigation at 1978 use rate. Area A is steady-state, area B is 50 years after irrigation pumping.

upwards. Flow E_2 leaves the barrel by gushing through the wedge. When the water level h rises above the bottom of the wedge, the flow through the wedge increases rapidly. The barrel furthermore has a hole in its bottom connected by a small pipe to a large tank also containing water. The direction of the flow D + F passing between the barrel and the tank depends upon their relative water levels. Flow I is removed from the barrel for use, and flow R is put into the barrel but cannot be controlled by the user of the water I. R is unknown, even the size of the barrel isn't known very accurately since the size of the aquifer and its storage coefficient S and/or specific yield S_y are not known very accurately. The flow E_2 leaving through the wedge cannot be measured except with considerable difficulty. The question to be answered is: How fast can water for use be removed from the barrel at a sustained rate? If D + F is ignored because it is small, then it follows that I cannot be larger than R for a sustained period of time. Thus the determination of R is fundamental. It is known that R sometimes increases abruptly during certain times of the year, especially after heavy rainfall. One could obtain a measure of R by comparing its effect upon the change in the water level h in the barrel as compared to the change produced by I which is known. This simple principal would work quite accurately if rates I and R were large compared with the other terms in (4), which could be the case for the sudden removal of water from the barrel and the likewise sudden recharge of water to the barrel. This principle for finding R loses its practicality somewhat when applied to an aquifer because observation-well data frequently cannot provide an accurate enough measure of the relative change in the amount of water in the aquifer. Thus, for example, because of the placement of the observation wells, several months of heavy irrigation pumpage might appear to have lowered the water level more than a recharge period had raised the water level, even though in fact the recharge was greater than the irrigation pumpage.

Notwithstanding this limitation of observation wells, water-level declines, when observed over several years, will tend to level off if irrigation pumpage is going to be sustainable. If no leveling off is evident, and the continued water-level decline apparently would cause reduced well yields, then it may be that the irrigation pumpage will not be sustainable.

RESULTS AND SUMMARY

The purpose of this study has been to predict the ability of the aquifer to supply water for irrigation. The aquifer was divided into two segments, model areas A and B of figure 2. The model obtained an approximate value of 23,000 acre-feet per year (2,768,000 cubic feet per day) for the yearly average recharge rate R to model area A. For area B, a value of 6,800 acre-feet per year (811,000 cubic feet per day) was obtained. These values correspond to 0.83 inch per year and 0.76 inch per year over the 527-square mile and 167-square mile model areas A and B respectively. The recharge rate R is thought to be unaffected by any stress placed on the aquifer due to pumpage, and was independent of the hydraulic head in the aquifer, in the model. According to the model, area A gains an additional inflow (-F) of 2,300 to 2,400 acre-feet per year along its perimeter, the smaller value occurring when the yearly average irrigation pumpage rate is zero, and the larger value when the irrigation pumpage rate is 9,800 acre-feet per year, the approximate rate for the year 1978. When area A is supplying irrigation water at the 1978 pumpage rate, the total amount of water coming into the aquifer, 23,000 + 2,400 = 25,400 acre-feet per year, exceeds the pumpage rate I = 9,800 acre-feet per year by 15,600 acre-feet per year. This excess water is discharged as evapotranspiration and base flow to the James River. These numbers imply that area A could supply irrigation water at a considerably higher rate than was supplied in 1978, or in other recent years.

For area B, the irrigation pumpage rate I, for 1978, was approximately 7,200 acre-feet per year. This is a higher rate than the 6,800 acre-feet per year obtained by the model for the yearly average recharge rate, R. The model, furthermore, predicts an outflow F from area B which cannot be reversed by irrigation pumpage. Also, with the 1978 placement of irrigation wells, the model predicts that drawdown in the hydraulic head due to irrigation pumpage cannot reverse or stop the discharge of water to the James River flood plain. It follows that the aquifer in area B is not expected to be able to sustain irrigation pumpage rates as large as were supplied in the year 1978, or other recent years. A time-varying model solution predicts that area B would be able to supply a yearly average pumpage rate of 7,200 acre-feet per year for perhaps as long as 50 years. Some of the irrigation wells, however, would be expected to go dry during this time period.

Area A, of figure 34, shows the hydraulic head that would be expected if 1978 irrigation pumpage rates were to be continued indefinitely. The average decline in the hydraulic head shown, below the hydraulic head for no pumpage, is approximately 2.9 feet. Area B, of figure 34, shows the hydraulic head that would be expected if 1978 irrigation pumpage rates were to be continued for a period of 50 years. The average decline in the hydraulic head shown, below the hydraulic head for no pumpage, is approximately 13.5 feet. The 6 model nodes, that would be expected to go dry during this 50-year period, are denoted by the symbol d in figure 34.

These results are approximate. The predictions for the yearly average recharge rate R, 23,000 and 6,800 acre-feet per year, for model areas A and B, are of primary importance, but are definitely subject to error due to the nature of the modeling process.

REFERENCES

Howells, L. W., and Stephens, J. L., 1968, Geology and water resources of Beadle County, South Dakota: Part II, Water resources: South Dakota Geological Survey Bulletin 18, 56 p.

Trescott, P. C., Pinder, G. F., and Larson, S. P., 1976, Finite-difference model for aquifer simulation in two dimensions with results of numerical experiments: U.S. Geological Survey Techniques of Water-Resources Investigations, Book 7, Chapter C1, 116 p.

page 49 follows

APPENDIXES

Appendix I

Steady-State Hydrologic Budget

An appropriate and generalized conceptualization, applicable to the total hydrologic system of this study, is shown in figure 3.

In a steady-state budget, storage water is insignificant and is not considered. The variables of figure 3 may be thought of as being the amounts of water (L^3) that flow during an average one-year period. More precisely perhaps, they should be thought of as the amounts of water that flow during a large time period. The hydrologic system should be approximately in a state of equilibrium before the beginning of the period. Irrigation practices, if any, should have begun many years before the beginning of the period and be roughly the same each year, so that drawdowns have stabilized except for yearly fluctuations and changes due to short periods of drought.

With no irrigation, $I = 0$, the water routing in figure 3 gives:

$$0 = R - (D + F) - E_2 \tag{1}$$

and

$$P = r + E_1 + R \tag{2}$$

where the first equation follows from the conservation of water in the aquifer. Combining (1) and (2) gives:

$$P = E_1 + E_2 + (r + D + F). \tag{3}$$

Note that conservation of water in the dashed box of figure 3 gives (3) directly. When the system with $I = 0$ is changed due to irrigation, the values of E_1, E_2, R, r, D, and F change to $E_1 + \Delta E_1$, $E_2 + \Delta E_2$, $R + \Delta R$, $r + \Delta r$, $D + \Delta D$, and $F + \Delta F$ respectively. The precipitation P, however, remains the same. Note that this notation is different than in equations (1-3) in the text.

Equations (1), (2), and (3) thus become:

$$I = (R + \Delta R) - (D + \Delta D + F + \Delta F) - (E_2 + \Delta E_2) \tag{4}$$

$$(P + I) = (r + \Delta r) + (E_1 + \Delta E_1) + (R + \Delta R) \tag{5}$$

and

$$P = (E_1 + \Delta E_1) + (E_2 + \Delta E_2) + (r + \Delta r + D + \Delta D + F + \Delta F). \tag{6}$$

Note that (6) does not contain I and, as does (3), follows directly from the conservation of water in the dashed box.

Subtracting (1), (2), and (3) from (4), (5), and (6) gives:

$$(I - \Delta R) = -(\Delta D + \Delta F + \Delta E_2) \tag{7}$$

$$I = \Delta r + \Delta E_1 + \Delta R \tag{8}$$

and

$$0 = \Delta E_1 + \Delta E_2 + \Delta r + \Delta D + \Delta F. \qquad (9)$$

From (7), the net increase in water removed from the aquifer due to irrigation, $I - \Delta R$, is equal to the decrease in water going to D, F, and E_2.

For this study, the evapotranspiration increase ΔE_1 in (8) is expected to be a major portion of I. The increase in recharge, ΔR, is relatively small in comparison with I, as is Δr. The quantity $\Delta E_1/I$ almost certainly exceeds 0.5, but is less than 1.0. Because the irrigation water is applied by sprinklers and usually during times of the growing season when evapotranspiration is high, this quantity could very likely be greater than even 0.95. ΔD, ΔF, and ΔE_2 are in effect caused by the lowering of the hydraulic head in the aquifer, due to the net increase in water removed from the aquifer for irrigation, $I-\Delta R$. Thus, ΔD, ΔF, and ΔE_2 are negative.

Rearranging equation (4) gives:

$$I - \Delta R = R - (D + \Delta F + F + \Delta F) - (E_2 + \Delta E_2). \qquad (10)$$

This basic equation states that the net amount of water removed from the aquifer for irrigation $(I - \Delta R)$ is equal to aquifer recharge R less water lost from the aquifer due to discharge to streamflow $(D + \Delta D)$ less water lost from the aquifer due to evapotranspiration $(E_2 + \Delta E_2)$. It expresses the steady-state budget for the aquifer, and is found by steady-state solutions of the numerical model. When there is no irrigation I, ΔR, ΔE_2, ΔD, and ΔF are zero.

Appendix II

Time-Dependent Hydrologic Budget

Equation (10) of appendix I is modified for the time-dependent case by including storage water:

$$(I - \Delta R) = R - (D + \Delta D + F + \Delta F) - (E_2 + \Delta E_2) - \Delta S. \tag{1}$$

This equation states that during some time interval Δt; the net amount of water removed from the aquifer for irrigation $(I - \Delta R)$ is equal to aquifer recharge R less water lost from the aquifer due to discharge $(D + \Delta D)$ less water lost to an adjacent aquifer $(F + \Delta F)$ less water lost from the aquifer due to evapotranspiration $(E_2 + \Delta E_2)$ less the change in the water in storage in the aquifer ΔS. It expresses the time-dependent budget for the aquifer, as is found by time-dependent solutions of the numerical model. When there is no irrigation I, ΔR, ΔE_2, ΔD, and ΔF are zero and ΔS has a different value than when these quantities are not zero and irrigation is present.

Also, for the aquifer of this study the flow of water to an adjacent aquifer $(F + \Delta F)$ is fairly small compared with the other terms in (10) of appendix I. From the steady-state equation (10) of appendix I with $(F + \Delta F) = 0$, $(I - \Delta R) = R - (D + \Delta D + E_2 + \Delta E_2)$. Because of the geometry of the aquifer and the placement of irrigation wells in the aquifer, it probably is not possible to lower the hydraulic head sufficiently that $(D + \Delta D + E_2 + \Delta E_2)$ is decreased to zero, causing the total amount of recharge water R to be available for irrigation, i.e. $(I - \Delta R) = R$. It may happen that when irrigation is at a maximum that water is still being lost from the aquifer by discharge to streamflow and evapotranspiration, i.e. $(D + \Delta D + E_2 + \Delta E_2) > 0$. In this case $(I - \Delta R) = R - (D + \Delta D + E_2 + \Delta E_2)$ could be considerably less than R, thus diminishing somewhat the importance of knowing R, and increasing the importance of understanding D and E_2.

☆ U. S. GOVERNMENT PRINTING OFFICE: 1985-565-440